REPUBLIC OF TURKEY
ISTANBUL GELISIM UNIVERSITY
INSTITUTE OF GRADUATE STUDIES

Department of Electrical and Electronics Engineering

DEVELOPMENT OF CLEANING CYCLE FOR EDS DUST REMOVAL TECHNIQUE FROM SOLAR PANEL

Master Thesis

Faten AL-Azzawi

Supervisor

Asst. Prof. Dr. Mahmoud HK ALDABABSA

Istanbul – 2024

THESIS INTRODUCTION FORM

Name and Surname	**:**	Faten Jabbar Mahdi Al- Azzawi
Language of the Thesis	**:**	English
Name of the Thesis	**:**	Development of Cleaning Cycle for EDs Dust Removal Technique from Solar Panel
Institute	**:**	Istanbul Gelisim University Institute of Graduate Studies
Department	**:**	Electrical and Electronics Engineering
Thesis Type	**:**	Master
Date of the Thesis	**:**	25/1/2024
Page Number	**:**	72
Thesis Supervisors	**:**	Asst.Prof. Dr. Mahmoud H. K. ALDABABSA
Index Terms	**:**	Artificial Intelligence (AI), Photovoltaic (PV) Systems, Dust & Clean PV panels, Renewable Energy, Deep learning, Convolutional Neural Network (CNN), Image processing.
Turkish Anstract	**:**	ED'ler için Güneş Panelinden Toz Giderme Tekniği Temizleme Döngüsünün Geliştirilmesi.
Distribution List	**:**	To the Institute of Graduate Studies of Istanbul Gelisim University To the National Thesis Center of YÖK (Higher Education Council)

Signature

Faten Jabbar Mahdi Al- Azzawi

REPUBLIC OF TURKEY
ISTANBUL GELISIM UNIVERSITY
INSTITUTE OF GRADUATE STUDIES

Department of Electrical and Electronics Engineering

DEVELOPMENT OF CLEANING CYCLE FOR EDS DUST REMOVAL TECHNIQUE FROM SOLAR PANEL

Master Thesis

Faten Jabbar Mahdi Al- Azzawi

Supervisor

Asst. Prof. Dr. Mahmoud HK ALDABABSA

Istanbul – 2024

DECLARATION

I hereby declare that in the preparation of this thesis, scientific ethical rules have been followed, the works of other persons have been referenced in accordance with the scientific norms if used, there is no falsification in the used data, any part of the thesis has not been submitted to this university or any other university as another thesis.

Faten Jabbar Mahdi Al- Azzawi

25/1/2024

TO ISTANBUL GELISIM UNIVERSITY

THE DIRECTORATE OF INSTITUTE OF GRADUATE STUDIES

The thesis study of Faten Jabbar Mahdi Al- Azzawi titled as (Development Of Cleaning Cycle For Eds Dust Removal Technique From Solar Panel) has been accepted as MASTER in the department of Electrical-Electronic Engineering by out jury.

Signature

Director *Asst. Prof. Dr. MAHMOUD H. K. ALDABABSA*

(Supervisor)

Signature

Member

Asst. Prof. Dr. HALIT YAHYA

Signature

Member

Asst. Prof. Dr. MOHAMMED SALEM

APPROVAL

I approve that the signatures above signatures belong to the aforementioned faculty members.

... / ... / 2024

Signature

Prof. Dr. İzzet GÜMÜŞ

Director of the Institute

SUMMARY

Solar panels play a crucial role in harnessing sunlight to generate electricity, but their efficiency is significantly impacted by many factors. The accumulation of dust on solar panels poses a challenge to energy production efficiency, particularly in regions with high dust rates such as the Middle East. Therefore, implement a PV dust detection system with high accuracy using optimization algorithms like Deep Learning (DL) is essential to enhance module efficiency, reduce maintenance costs, and promote resource conservation. This project introduces a novel approach using DL and image processing to develop a dust detection system for solar panels. Leveraging Convolutional Neural Network (CNN) algorithms, the study aims to fine-tune model parameters for effective dust detection and classification. The overarching goal is to enhance module efficiency, reduce maintenance costs, and optimize resource utilization. The dataset images were cleaned, augmented, and filtered utilizing image processing tools. Then, the dataset was categorized into two classes namely clean, and dusty with training and validation processes of ratio 80% of total images (2049 images), and testing and validating with 20% of total images (513 images) were used for validation and testing processes as (307 images) for validation and (206 images) for testing. Three predefined DL algorithms which are (Inception-v3, VGG-16, and Resnet-50) and the proposed DL that is called Efficient-net were developed and implemented within this work. The proposed Efficient-net outperforms the other three techniques in high accuracy with 87% rather than Inception-v3 with 84%, VGG-16 with 72, and Resnet-50 with 80%.

Key-Words: Artificial Intelligence (AI), Photovoltaic (PV) Systems, Dust & Clean PV panels, Renewable Energy, Deep learning, Convolutional Neural Network (CNN), Image processing.

ÖZET

Güneş panelleri, elektrik üretmek için güneş ışığından yararlanmada çok önemli bir rol oynar, ancak verimlilikleri birçok faktörden önemli ölçüde etkilenir. Güneş panelleri üzerinde toz birikmesi, özellikle Orta Doğu gibi toz oranının yüksek olduğu bölgelerde enerji üretim verimliliği açısından zorluk teşkil etmektedir. Bu nedenle, Derin Öğrenme (DL) gibi optimizasyon algoritmalarını kullanarak yüksek doğrulukta bir PV toz algılama sistemi uygulamak, modül verimliliğini artırmak, bakım maliyetlerini azaltmak ve kaynak korumasını teşvik etmek için çok önemlidir. Bu proje, güneş panelleri için bir toz algılama sistemi geliştirmek üzere DL ve görüntü işlemeyi kullanan yeni bir yaklaşım sunmaktadır. Evrişimli Sinir Ağı (CNN) algoritmalarından yararlanan çalışma, etkili toz tespiti ve sınıflandırması için model parametrelerine ince ayar yapmayı amaçlıyor. Kapsamlı amaç, modül verimliliğini artırmak, bakım maliyetlerini azaltmak ve kaynak kullanımını optimize etmektir. Veri kümesi görüntüleri, görüntü işleme araçları kullanılarak temizlendi, genişletildi ve filtrelendi. Daha sonra veri seti temiz ve tozlu olmak üzere iki sınıfa ayrılarak toplam görüntülerin %80'i (2049 görüntü) oranında eğitim ve doğrulama işlemleri yapılmış ve doğrulama için toplam görüntülerin %20'si (513 görüntü) ile test ve doğrulama işlemi kullanılmış ve doğrulama için (307 görüntü) ve test için (206 görüntü) test süreçleri. Bu çalışma kapsamında önceden tanımlanmış üç DL algoritması (Inception-v3, VGG-16 ve Resnet-50) ve önerilen Efficient-net adı verilen DL geliştirilmiş ve uygulanmıştır. Önerilen Efficient-net, %84 ile Inception-v3, 72% ile VGG-16 ve %80 ile Resnet-50'ye kıyasla %87 ile diğer üç tekniği yüksek doğrulukta geride bırakıyor.

Anahtar Kelimeler: Yapay Zeka (AI), Fotovoltaik (PV) Sistemler, Toz ve Temiz PV paneller, Yenilenebilir Enerji, Derin öğrenme, Evrişimsel Sinir Ağı (CNN), Görüntü işleme.

TABLE OF CONTENTS

CHAPTER FOUR
EXPERIMENTIAL RESULTS

ABBREDIVATIONS

AI	**:**	Artificial Intelligence
ANN	**:**	Artificial Neural Networks
CNN	**:**	Convolutional Neural Networks
DF × DF	**:**	Feature Map Size
f(i,j)	**:**	Noisy Image
FF	**:**	Fill Factor
g(i,j)	**:**	Filtered Image
F1-Score	**:**	Average of Recall and Precision
FN	**:**	False Negative
FP	**:**	False Positive
GIF	**:**	Graphics Interchange Format
H-GRNN	**:**	Hierarchical Generalized Regression
IS	**:**	Short circuited solar cell current
JPEG	**:**	Joint Photographic Experts Group
M	**:**	Number of Input Channels
MLP	**:**	Multilayer Perception
MTCNN	**:**	Multitask Cascaded Convolutional
N	**:**	Number of Output Channels
Dk × Dk	**:**	Kernel Size
PNG	**:**	Portable Network Graphics
ReLU	**:**	Rectified Linear Unit
RMSE	**:**	Root Mean Square Error
RNN	**:**	Recurrent Neural Networks
TIFF	**:**	Tag Image File Format
TN	**:**	True Negative
TP	**:**	True Positive
TL-VGG16	**:**	Transfer Learning Network
VGG16	**:**	Visual Geometry Group 16-layer model
VOC	**:**	Open circuited solar cell voltage

LIST OF TABLES

LIST OF FIGURES

PREFACE

Throughout the process of preparing and writing this thesis, I express my gratitude to **Asst. Prof. Dr. Mahmoud HK ALDABABSA** for the support rendered and to the members of the Thesis jury for their valuable comments and suggestions that assisted in managing and advancing the thesis. Last but not least, my sincere appreciation goes to my family for their support.

INTRODUCTION

This research addresses the critical challenge of dust accumulation on solar panels, a major impediment to their efficiency in electricity generation, especially in regions with high dust rates such as the Middle East. The study focuses on implementing a Photovoltaic (PV) dust detection system utilizing advanced optimization algorithms, specifically Deep Learning (DL). By leveraging Convolutional Neural Network (CNN) algorithms, the research aims to fine-tune model parameters for effective dust detection and classification. The overarching goal is to enhance module efficiency, reduce maintenance costs, and optimize resource utilization in solar panel installations. This work introduces a novel approach that combines DL and image processing techniques to develop a robust dust detection system. The study evaluates three established DL algorithms (Inception-v3, VGG-16, and Resnet-50) and introduces a novel DL technique named Efficient-net, with the latter demonstrating superior performance with a good accuracy and other perfomance metrics. This research contributes to the advancement of efficient and cost-effective solutions for maintaining optimal solar panel performance in challenging environmental conditions.

CHAPTER ONE
INTRODUCTION

1.1 Introduction

Electrical energy resources can primarily be divided into three groups: nuclear, fossil and renewable energy resource. There are many renewable energy sources (RES) including hydroelectricity, marine energy, biomass, geothermal energy, solar cells energy and wind energy, which supply 14% of the total global energy (Kabalci et al.,2015&Panwar et al.,2011). A renewable energy studies the reduction of fuels and the effects of the greenhouse. Clean systems with no fuel demands, reliability and sustainability of solar photovoltaic systems (PV) are now significant in RES systems (Mahela&Shaik,2017).

The problems of energy shortages and environmental pollution in recent years contribute led to renewable energy demand is increasing, which are replenished naturally in the sunlight, rain, wind, waves, tides and geothermal heat on a timescale. Technologies of renewable energy need less overall maintenance, unlike generators that use traditional fuel sources, emitting no noise and has many advantages in the coming stage, it is necessary to introduce such a mixture of energy to support the electrical network, which suffers from excessive consumption by the consumer of all types, whether this sector is residential, industrial, commercial, or agricultural.

PV energy source technologies depend on power electronic devices. So, power electronics is very significant today because it is concerned with the control and conversion of electrical power. That using power semiconductor devices operate in switching mode and thus with advanced technology the efficiency of power electronic devices can be approached to (95%), power electronics costs decrease, the size is reduced and reliability is increased with longer life and better performance (Panwar et al.,2011). PV power system researches are the biggest focus today include the DC-DC converter design, inverter design, material of modules and reliability of the system among other (Bose,2010).

The smallest segments of the photovoltaic array are photovoltaic cells, which are gathered into photovoltaic modules. At this point, as configuration series-parallel connection, photovoltaic modules will set as a photovoltaic array, next developed to the photovoltaic energy plants (Mahela&Shaik,2017). Photovoltaic cell consists of two semiconductor junctions, in which one is dopped P-type and the other is dopped N-type. At the point

when these two semiconductors are placed related, a dissemination procedure happens between the electrons of the N-type and the gaps of the P-type, which results in an exhaustion region and an electric field over this region as appeared in Figure 1.

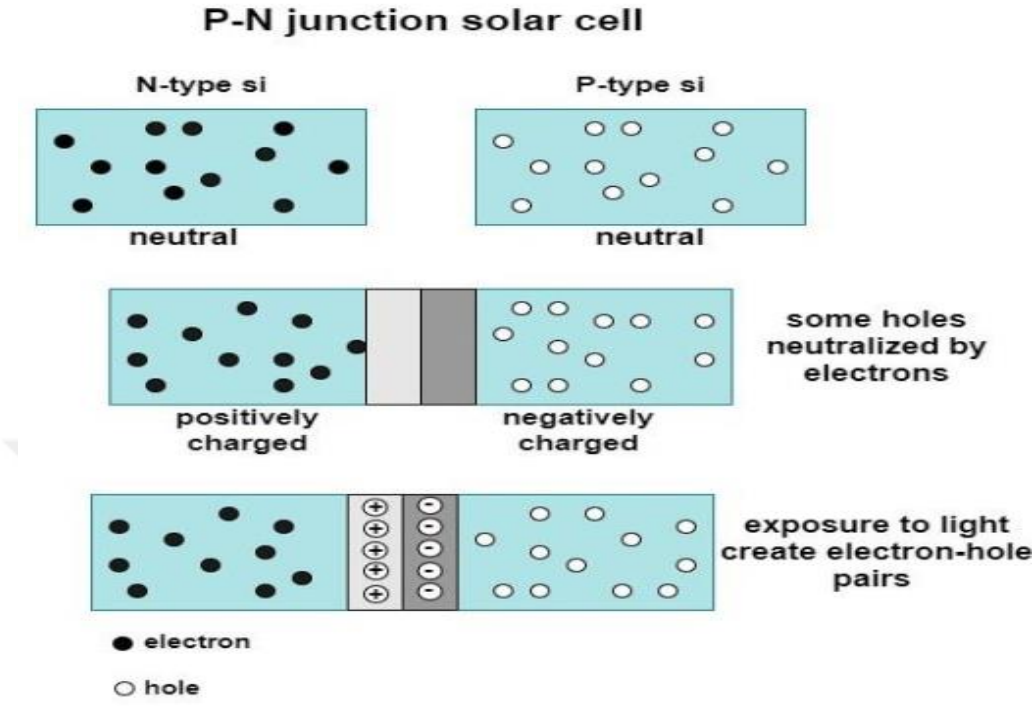

Figure 1. The P-type and N-type semiconductors connection resulting process.

Sunlight is composed of photons, when solar irradiation with a suitable wavelength is absorbed by the photovoltaic cell, the photon energy is transferred to the electron in a semiconductor material. So, that is enabled the electron to jump in a higher level of energy is called conduction band, these electrons in the conduction band are free to move in the material. The movement of electrons causes the creation of DC current in a PV cell. Lastly, the positive charges are assembled in the P-type semiconductors and the negative charges are assembled in the N-type semiconductors. At the ends of the photovoltaic cell creates a difference of potential, the Figure (1-2) displays the creation of photovoltaic cell silicone. The upper surface of the photovoltaic cell consists of a small layer of p-type materials so that lighting can arrive easily at the material. Metallic rings situated around the material of P-type and N-type, which operate as the positive and negative output terminals respectively as shown in Figure (2) (Li,&Zheng,2011).

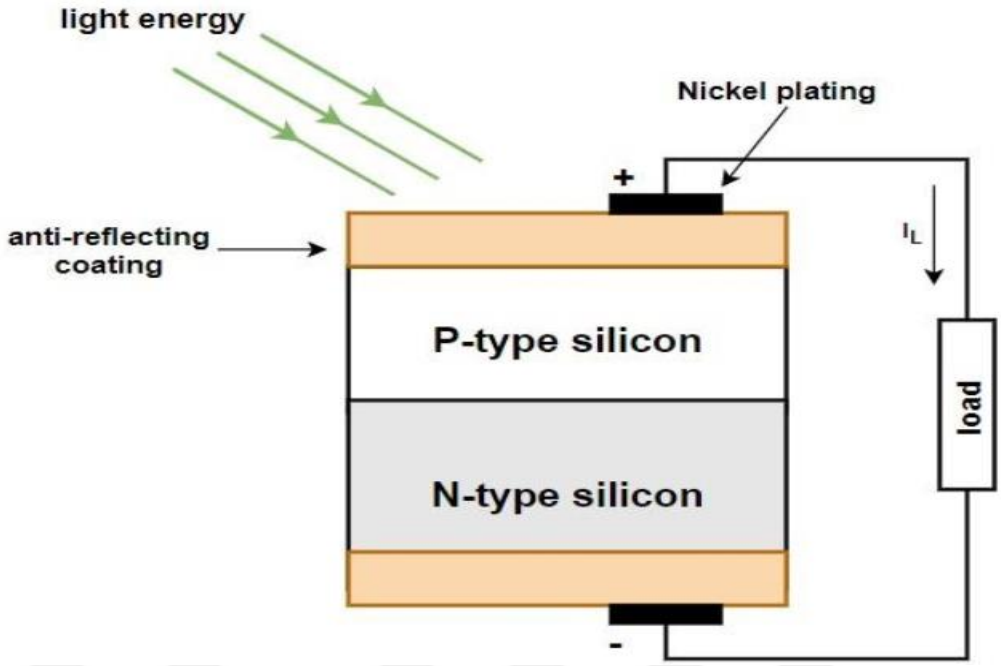

Figure 2. A principle of photovoltaic cell operation.

It should be mentioned that part of the sun's radiation is reflected on the surface of PV cell. Such reflected radiation is not converted into electrical energy and only the radiation absorbed by the photovoltaic cells is of importance to us. The PV module or solar panel is a simple unit, which can provide higher voltages and produce extra power than just one cell. A PV module contains several cells that are interconnected and laminated together, a commonly used to protect the crystalline-based photovoltaic cells are sandwiched by the substrate of tempered glass as shown in Figure (3). For series interconnection from the top to the bottom of PV cells, metal conductors are connected. Manufacturing companies nowadays are interested in cost-effective solutions and provide all several sizes of solar panels: such as 48, 54, 60, or 72 cells (Xiao,2017).

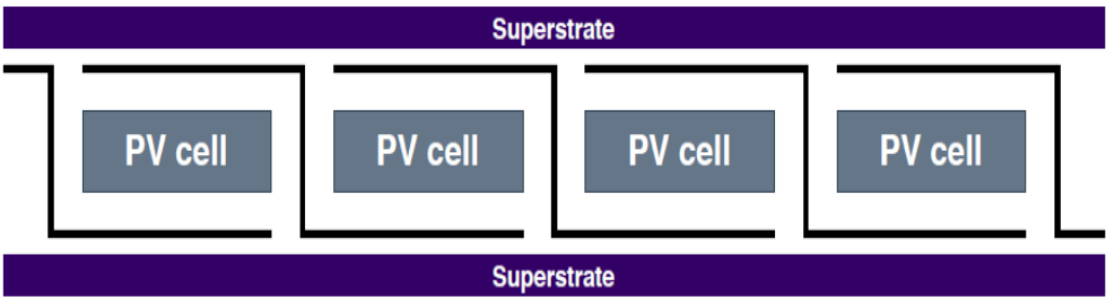

Figure 3. Layer of photovoltaic module cells.

1.2 Equivalent circuit of the PV cell

In this work, and to obtain the characteristics of the PV system, an analytical methodology will be used. Many circuit equivalent models have been created and suggested in the literature to provide a real explanation of the characteristics of the PV panel and the model of a single diode is the most widely used. Five parameters must be considered in the model, i.e. light produced current (I_l), the leakage/reverse saturation current (I_o), the diode quality factor (n), the series resistance (R_s) and the shunt resistance (R_{sh}), can be defined as complete characteristics of a photovoltaic cell in a single diode model. I_l and Io may be considered to be external factors while the others are internal factors. A PV cell's characteristics are under solar irradiance is given in terms of photovoltaic cells output current(I) and photovoltaic cell voltage (V) (Askarzadeh&Rezazadeh, 2012; Rusirawan&Farkas, 2014). The electric equivalent circuit diagram is shown in Figure (4) is the PV cell model of a single diode, which consist of a photo current source, single diode, shunt resistance and series resistance.

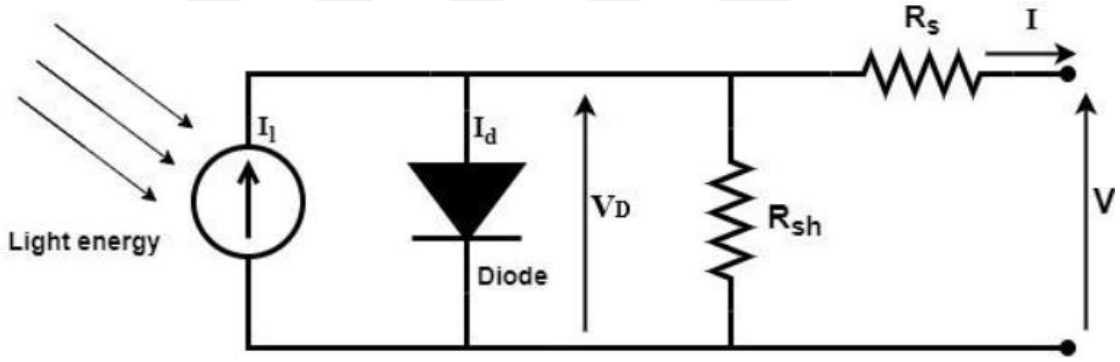

Figure 4. PV cell model of single diode.

The simple equation defining the I, V, P characteristics of the model of PV cell can be described based on Kirchoff's First Law and written by equation (1-1).

$$I = I_1 - I_D - I_{sh} \quad (1\text{-}1)$$

$$I_D = I_o \left[\exp\left(\frac{V + IR_S}{\frac{nKT}{q}} \right) - 1 \right] \quad (1\text{-}2)$$

and in the expression of the model of a single diode (five model parameters) can write equation (1-2) as:

$$I = I_1 - I_o \left[\exp\left(\frac{V + IR_S}{\frac{nKT}{q}} \right) - 1 \right] - \frac{V + IR_S}{R_{sh}} \quad (1\text{-}3)$$

Where I_l is a photo current, I_o is the diode saturation current, q is the charge of an electron (q = 1.60217657 $\times 10^{-19}$ Coulombs), V is the photovoltaic panel output voltage, *I* is the

photovoltaic panel output current, k is a Boltzmann's constant (k = 1.3806488 $\times 10^{-23}$ Joules per Kelvin), T_c is the working temperature of the cell, n is a diode quality factor, R_s is the series resistance and R_{sh} is the shunt resistance. Experiments indicate a drop in the output voltage through increasing series resistance, while a reduction in the shunt resistance decreases the output current. It has shown that by increasing the series resistance from (0.36Ω to 1.80Ω), both the Maximum Power (Pmax) and the Fill Factor (FF) is decreased by 25%, it clear that the value of resistance affected on the model produces (Rusirawan&Rezazadeh,2012). The relation between Pmax and FF stated by equation (1- 4):

$$FF = Fill\ Facctor = \frac{P_{max}}{V_{oc} \times I_{sc}} = \frac{V_{max} \times I_{max}}{V_{oc} \times I_{sc}} \quad (1\text{-}4)$$

Where, V_{oc} is the open circuited solar cell voltage, while I_{sc} is short circuited solar cell current. Both $V_{oc}$and I_{sc} are always larger than V_{max} and I_{max}.

In practice, the series resistance of a simplified model is low (≈ 0), the shunt resistance is high (≈ ∞) but also the diode quality factor equal n to 1 (even though the quality factor of a diode depends on the type of the material), so their effects are ignored. In this relation, with regard to R_s = 0=short circuited (so small) and R_{sh} = ∞=open circuited (so high) as referring to above statements, the equation (1-5) can be rewritten by:

$$I = I_1 - I_o \left[\exp\left(\frac{V}{\frac{nKT}{q}} \right) - 1 \right] \quad (1\text{-}5)$$

$$P = VI_1 - VI_o \left[\exp\left(\frac{V}{\frac{nKT}{q}} \right) - 1 \right] \quad (1\text{-}6)$$

1.3 Photovoltaic panels types

Photovoltaic cells can be constructed from different materials in many different ways. Even so, they all do the same job of collecting and converting solar energy into useful electricity. Silicon is the most used material for solar panel construction. Many of these solar cells are needed to implement solar panels and many panels composite photovoltaic arrays. The advancement of manufacturing depends on the development of structures and materials but the aim is always maximum power at a minimum cost. The world market is dominated by three types of PV cell technology: monocrystalline silicone, polycrystalline silicone and thin film. The high cost and higher-efficiency PV technology, which includes gallium arsenide and multi-junction cells, is less popular but

is suitable for use in concentrated photovoltaic systems and applications of space. Several emerging photovoltaic systems technologies include Perovskite cells, dye-sensitized solar cells, organic solar cells and quantum dots which are useful insights and guidelines for defining a pathway for future photovoltaic designs towards clean and sustainable energy generation (Ibn-Mohammed et al.,2017). In many ceiling-integrated applications, strings are encapsulated (usually within the glass) to shape a module (usually referred to as a "panel"). The PV panel is the main building block of the PV system and that any numbers of panels can be connected together to provide the desired electrical output.

The first generation of PV technology consists of a crystalline structure that uses silicon (Si) to manufacture solar cells that are combined to create PV modules. However, this technology is not obsolete, rather it is constantly being improved to develop its capacity and performance as shown in Figure (5).

1.3.1 Mono-crystalline photovoltaic cells

As shown in figure (5)(a), this type is a commonly used type of cell that contributes to about 80% of the market and remains leading up to extra efficient and cost effective PV technologies. It mainly the crystalline (Si) is the PN-junction. To manufacture the monocrystalline silicon, a single crystal ingot, is cultivated by using the method of Czochralski. Monocrystalline silicone solar cells had a maximum efficiency of around 23% under standard test conditions (STC). By using other types of semiconductor materials, the efficiency can reach 30% under STC (Chaar&Zein,2011).

1.3.2 Poly-crystalline photovoltaic cells

In order to change the efficiency, the photovoltaic industry has been working on new crystallizing techniques. Such technology as illustrated in Figure (5)(b) has become ever more desirable as production costs but lower efficiency (15%) of these cells than the monocrystalline. Melting and solidifying silicone is used to orient the crystals in a constant direction that produces a rectangular ingot of multicrystalline silicone and is eventually cut into blocks and finally into thin wafers. The cultivation of wafer-thin ribbons of polycrystalline silicone, however, may abolition this final step. Evergreen Solar developed this technology (Chaar&Zein,2011).

1.3.3 Thin film photovoltaic cells

When compared to crystalline silicone cells, the technology of thin film as in Figure (5)(c) promises to decrease the cost of photovoltaic arrays by decreasing the materials and production without jeopardizing the lifetime of cells and the danger to the environment. Unlike the crystalline form of solar cells, where pieces of semiconductors are sandwiched between the glass panels to create the modules, (Akarslan,2012) the fact that the layers are much thinner caused by less photovoltaic material to absorb a radiation form the sun, hence the efficiency of thin-film solar modules is lower than crystalline. As commercial importance, four kinds of thin-film cells that appear are: the amorphous silicon cell, the copper indium diselenide/cadmium sulphide heterojunction cell, thin polycrystalline silicone on a low-cost substrate and cadmium telluride/cadmium sulphide heterojunction cell (Akarslan,2012).

(a) **(b)** **(c)**

Figure 5. Types of photovoltaic panel (a) Mono-crystalline (b) Poly-crystalline (c) Thin-film.

1.4 Photovoltaic system architecture

There are three types for grid-connected solar energy systems:

- Central inverter systems
- String inverter systems
- Micro-inverter systems

1.4.1 Central inverter system

The central inverters in large PV facilities, as illustrated in Figure (6) (a), have their own maximum power point tracker (MPPT) algorithm. They are installed in the central inverter in the case of PV installations. Large solar PV facilities are made up of strings of PV panels linked in series and parallel. Each string of PV panels is linked to a central inverter. Connection to a central inverter has various drawbacks, including as the need for high voltage DC cabling, which creates cable losses throughout the system. When the PV system is partially shaded, it may be totally deactivated (Kjaer et al., 2020).

1.4.2 String inverter system

Figure (6) (b) depicts a string inverter connected to a single PV string. Rows of solar panels are placed. This allows for individual MPPT control for each string. Each photovoltaic string transports the direct current (DC) electricity generated by the solar panels to the string inverter. If the system uses string inverters and a single panel is shadowed for a part of the day, the performance of each panel in the PV string is decreased to the level of the struggling panel. As a result, this is insufficient to address shading issues in the PV system. When the performance of Micro-inverter systems was compared to string inverter systems under different shading situations, the findings showed that Micro-inverter systems performed better for both shadow and non-shadowing PV panels (Famoso et al.,2015).

1.4.3 Micro-inverter system

As can be seen in Figure (6) (c), a Micro-Inverter connected to the single PV module is a trend in residential grid-connected photovoltaic systems that replaces a single inverter connected to a series of connected PV modules (string) for various reasons such as: (1) power harvesting improvement; (2) increased energy efficiency; (3) lower cost of installation; (4) increased flexibility and modularly; (5) plug and play operation. It was found that the extra micro-inverter energy harvest gives economic benefits over the expected lifetime of the PV systems, especially when taking into account the cost of changing the string inverter. A photovoltaic (PV) of low power inverter connected to one PV module is a micro-inverter. Instead of direct current (DC), the PV module generates alternating current (AC). As the relatively low cost and modular design, it can be connected several micro-inverters in parallel to increase the power rating.

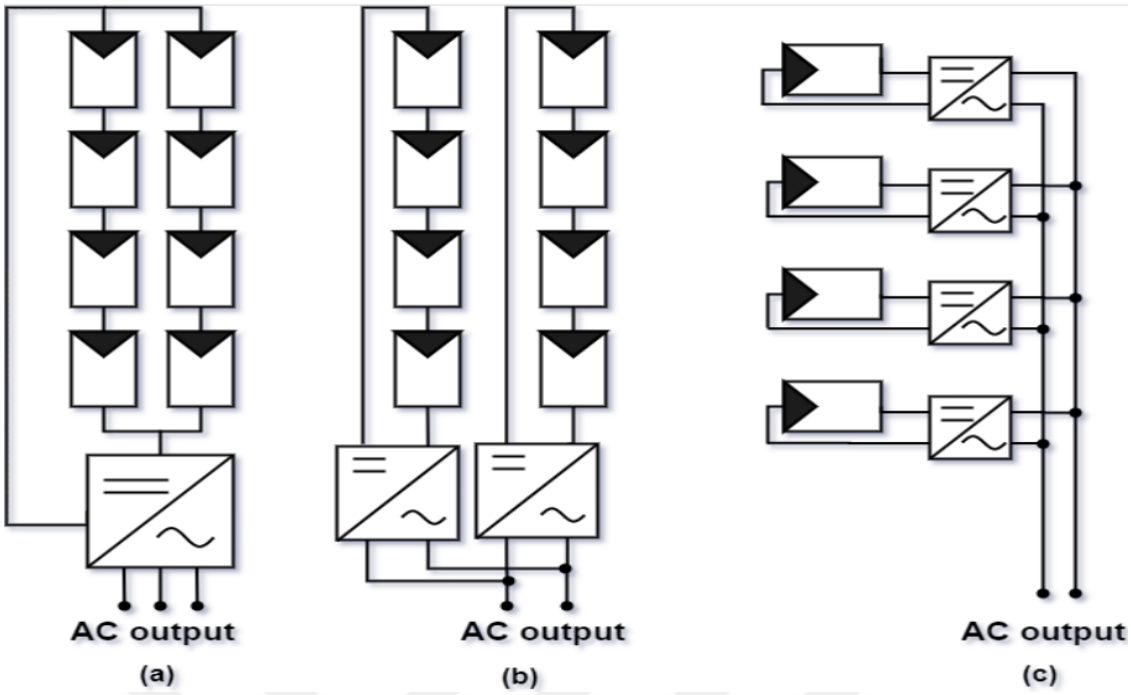

Figure 6. PV connected systems architectures: (a) central inverter system (b) string inverter system (c) Micro-inverter system.

1.5 Power processing stages

A photovoltaic system mainly consists of PV panels that generate DC power from PV and an inverter whose main role to convert the DC power into AC power then injected the utility grid. A PV system can also be classified in the terms of power processing stages according to this classification.

1.5.1 Single-stage inverter system

Figure (7) show the single-stage system. In the inverter stage, all tasks will be performed which include MPPT, voltage regulation, voltage amplification if needed and control of grid current. The benefits of using one power stage are the component number reduction and small switching losses of transistors at the inverter stage (Rodriguez& Balda,2013). Where PLL: is the phase-locked loop & MPPT CTRL: is the maximum power point control.

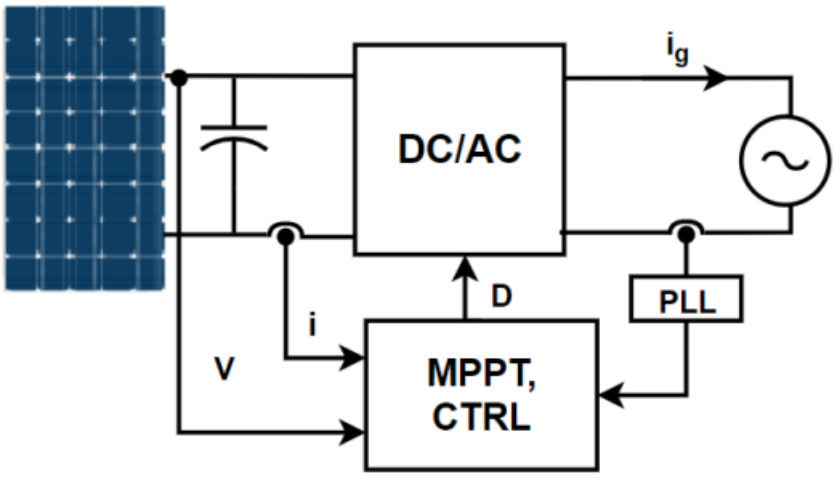

Figure 7. Single stage inverter system.

1.5.2 Dual power processing stage inverter system

The most common configuration for a multistage system employs two power processing stage. One of these two processing stages is a DC-DC converter, which steps up the PV panel voltage to a suitable DC value, handles MPPT, and its output is DC voltage, while the other is a DC-AC inverter, which controls grid current using pulse width modulation. One of the key advantages of the two-stage micro-inverter depicted in Figure (8) ((Mustafa,2017) is its capacity to supply reactive power that may be utilized for power factor adjustment in distribution systems.

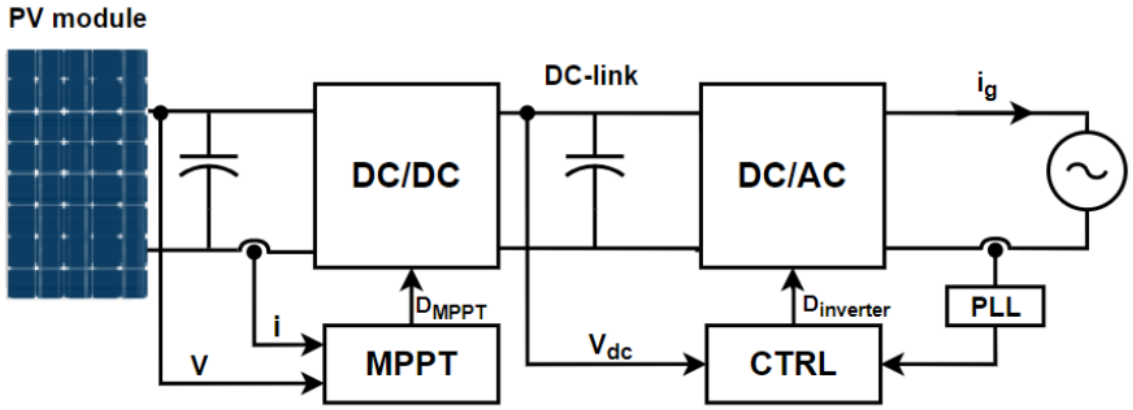

Figure 8. Dual power processing stage inverter system.

1.5.3 Dual-stage inverter system with two DC-DC converter

Each DC-DC converter stage's function is to perform MPPT and potentially amplification. As illustrated in Figure (9), each PV module or PV string is linked to a particular DC-DC converter, which is coupled to a common inverter. PV arrays' features

vary from one another. In high-power configurations, it may comprise more than one DC-C converter, one for each PV array. Despite the fact that they include several DC-DC converters, these systems are referred to as two-stage. The DC-DC converter stage regulates the DC-link voltage and controls the maximum power point tracking(MPPT) (Mirhosseini et al.,2014).

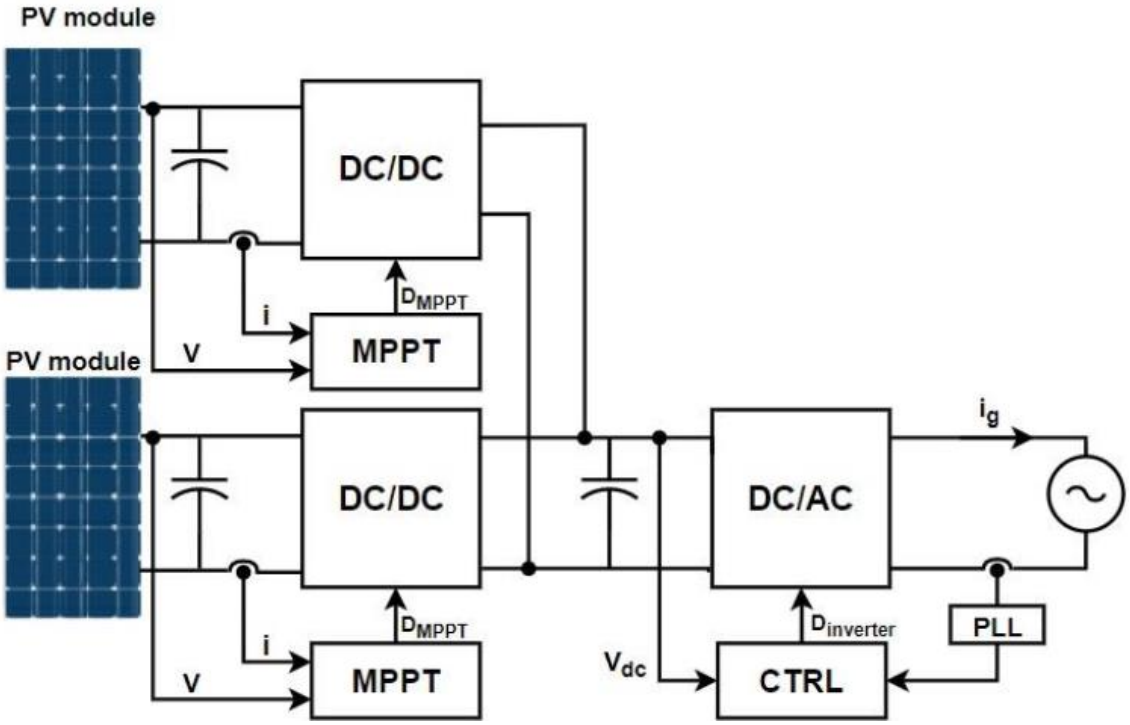

Figure 9. Dual stage inverter system.

1.6 Problem Statement

Solar panels are indispensable for harnessing sunlight to generate electricity, but their efficiency is significantly compromised by various factors. One prominent challenge is the accumulation of dust on solar panels, particularly in regions with high dust rates like the Middle East. This dust accumulation adversely affects energy production efficiency, leading to reduced module efficiency, increased maintenance costs, and suboptimal resource utilization. To address this issue, there is a critical need for the development and implementation of a high-precision Photovoltaic (PV) dust detection system. The existing methodologies for dust detection often fall short in terms of accuracy and effectiveness. Therefore, this project seeks to employ state-of-the-art optimization algorithms, specifically Deep Learning (DL) techniques, to enhance the accuracy of the dust detection system. The proposed solution leverages Convolutional Neural Network (CNN)

algorithms, with a focus on fine-tuning model parameters to achieve effective dust detection and classification.

1.7 Thesis objectives

The main objective of the thesis is:

1. Present a mathematical solar irradiation model and technique for predicting PV output power for various PV system sizes and orientations.
2. Discusses the approach for detecting dust on PV panel surfaces, including image processing.
3. Using optimization strategies, create a deep learning model for dust detection on solar panel surfaces that achieves the best detection accuracy.
4. Make use of the AI system for computational and logical operations.
5. Enhance module efficiency, reduce maintenance costs, and promote resource conservation.

1.8 Thesis outline

This thesis consists of five chapters as:

Chapter 1: Introduction

- Overview of electrical energy resources.
- Significance of renewable energy sources (RES).
- Renewable energy studies and the role of solar photovoltaic systems (pv) in clean, reliable, and sustainable energy.
- Give the solar cell equivalent circuits, microgrid PV system and its components.

Chapter 2: Literature Review

- Rapid development and research in pv solar systems.
- Review of selected works by individuals or companies.
- Identification of known issues addressed in each review.

Chapter 3: Methodology

- Presentation and elaboration of main concepts in the framework.
- Discussion of image preprocessing, feature extraction methods, classification approaches, model performance metrics, and models evaluations.

Chapter 4: PV Dust Detection in Deep Learning

- In-depth presentation and elaboration of main concepts in the framework.

- Discussion of image preprocessing, feature extraction methods, deep learning classification approaches, model performance metrics, and models evaluations.
- Implementation of systems for accurate classification of local and global pv panel images (clean and dusty classes).
- Use of CNN with RESNET, VGG-16, INCEPTION-3, and NETB0 deep learning architectures.
- Dataset acquisition and classification for local and global PV panel images.
- Evaluation of performance metrics for testing and assessment.

Conclusion and Discussion

- Summarization of key findings and insights.
- Identification of achievements and limitations.
- Proposals for future research and development.

CHAPTER TWO
LITERATURE REVIEW

2.1 Introduction:

PV solar systems are seeing a significant surge in development and research. A literature study of some chosen relevant works done by people or corporations in which the developed work has been inspired by and attempted to solve certain recognized challenges that are described in each review follows.

2.2 Historical Review:

The sun is a massive source of energy; the earth's surface gets enough energy from the sun in one hour to supply the earth's energy demands for one year (Messenger, et al., 2018). The earliest reported solar energy technology was utilized to power the first space satellites in the 1950s (Shubbak,2019). Because of its relatively expensive cost at the time, solar energy was confined to space applications in the early phases of technology. Nonetheless, the solar energy sector has grown dramatically in recent years. For example, in 2010, 17 GW of new solar fields were installed globally, raising the overall capacity of the PV industry to 40 GW (Jager-Waldau,2021), as shown in Figure (1). In comparison to 2020, more than 130 GW of PV modules have been deployed worldwide (Jaber,2021).

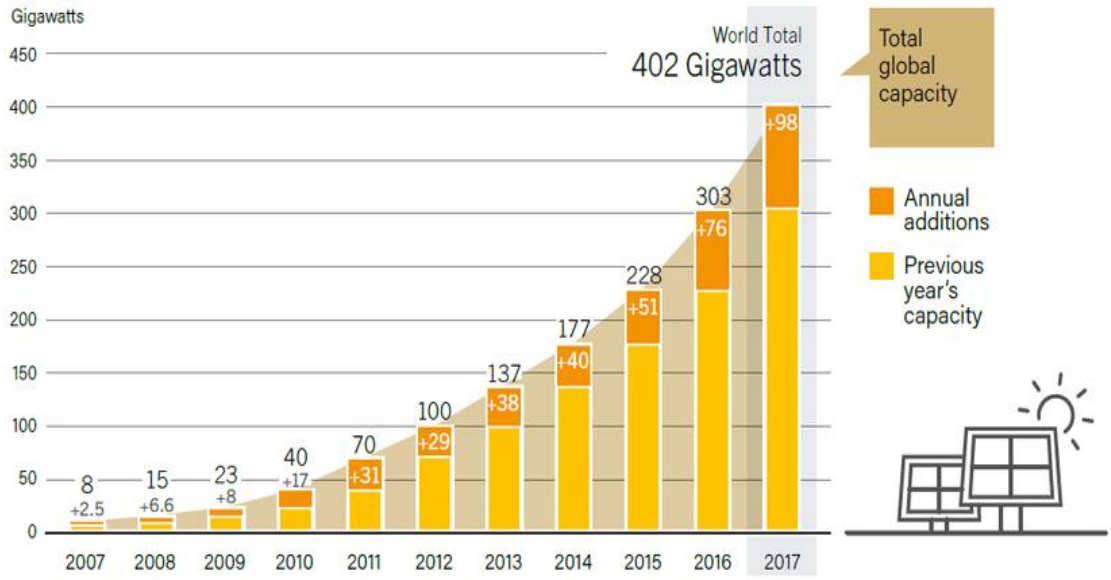

Figure 10. Cumulative installed PV fields from 2007 to 2017(Jager-Waldau,2021).

Recent studies have focused on grid interface behavior, control structure performance, and improving current topologies under operational settings. Because the integration of renewable energy systems to the grid is dependent on the power scale for which it is used, various researchers from various countries have been working since the dawn of this technology to improve power quality, efficiency, and stability using a variety of methods and techniques.

2.3 Relationship between Dust Level to the PV Characterstics

The collection of dust on the surface of PV panels is widely acknowledged to have a negative influence on power generation; nevertheless, there are no standardized equations that correctly characterize this link. This connection was formed by a thorough survey investigation on the performance of PV panels in the presence of collected dust (Yfantis&Fayed,2014;Roumpakias&Stamatelos,2020) since it is essential to complete the development of the intelligent detecting tool in this work. Figure (2) shows two PV panels with varied cleaning conditions.

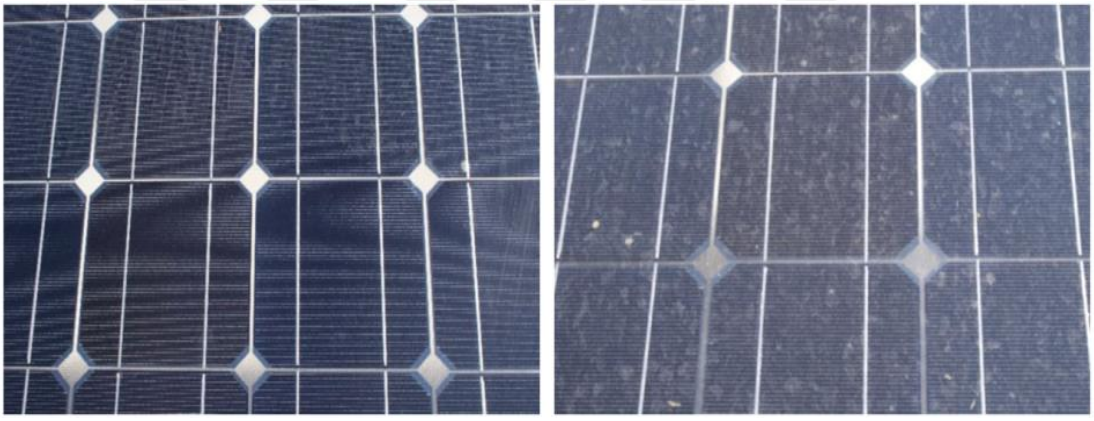

Figure 11. PV panels to study the impact of soiling on the output power: (left) cleaned PV panel and (right) dirty PV panel (Yfantis,2014)

Figure (3) illustrates the average produced power (in W) for a normalized dimension of a photovoltaic (PV) system at different levels of particle concentration (in g/m^2) found in prior research (Shaaban et al., 2020;Wu et al., 2020). Notably, the PV output power was transformed to % values (with the maximum power acting as the rated power) to verify that the derived formula was applicable to any size and mix of PV panels and arrays.

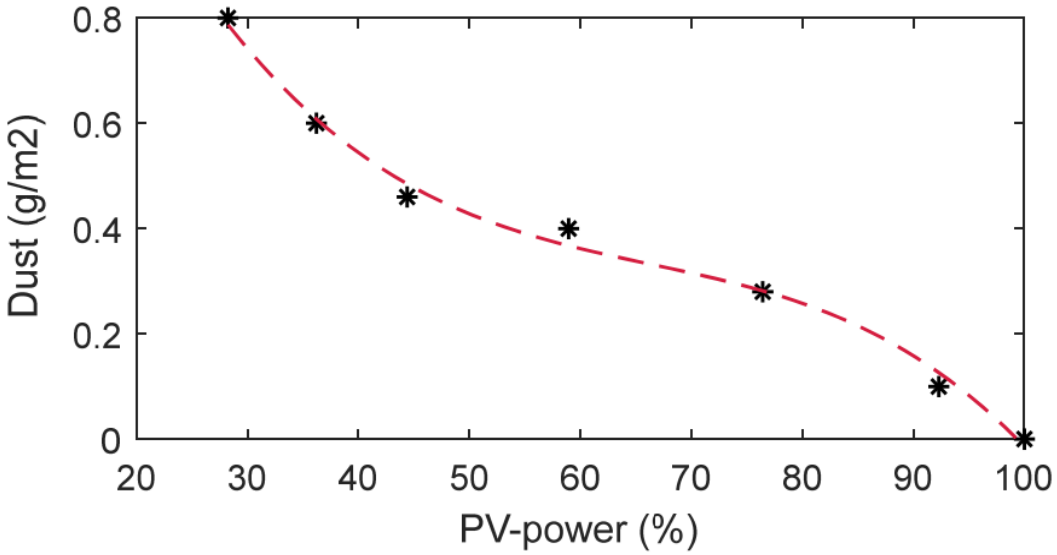

Figure 12. Dust weight as a proportion of normalized PV output power (Shaaban et al.,2020)

The accumulation of dust has an adverse impact on the performance of solar panels due to optical attenuation. Specifically, the interaction of electromagnetic radiation with solid dust particles in the external environment causes the radiation to be attenuated. Attenuation is calculated as the product of various types of interactions, including absorption, elastic scattering, and inelastic scattering (Mohammad et al., 2016). An illustration of the ISC generation over the course of a day is depicted in Figure (4). When the new mechanism (clean PV) is implemented, Isc generation remains at a greater level than when it is not utilized. During the course of the day, an approximate 0.8 Isc difference exists between the two scenarios. The proposal increases solar panel efficacy by over fifty percent.

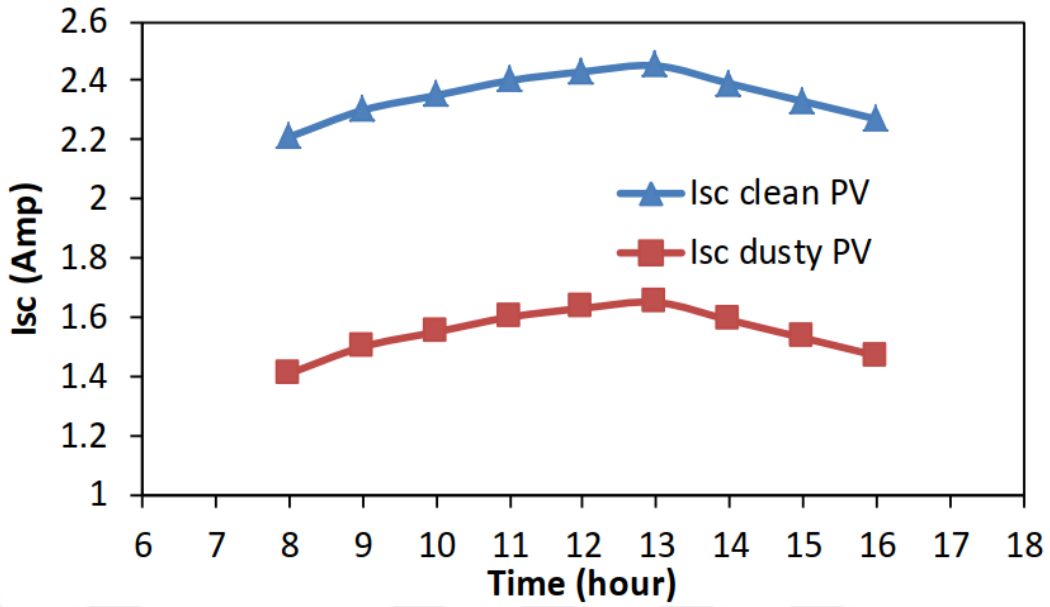

Figure 13. The PV short circuit current Isc .vs. daily time(Mohammad et al.,2016)

2.4 Literature Review:

In (Qasem et al., 2016), Dust accumulation on PV modules is a major hindrance to solar technology adoption, particularly in dust-prone regions such as the Middle East. To address this, the study presents an innovative approach using image processing to assess and manage dust on PV surfaces. High-resolution drone images are processed using a unique algorithm to detect and quantify dust levels. The method is validated against electrical measurements, with a detection variation of 5% to 5.5% based on the algorithm used.

In (Mohammed et al., 2018), Solar energy has become a popular choice due to its sustainability However, in Iraq, the efficiency of solar panels is often hampered by dust and dirt accumulation, particularly during sandstorms. This study offers a solution to this problem by introducing a method that continuously monitors power generation and automatically cleans the solar panels when needed. Using an Arduino Uno microcontroller and a windscreen wiper, the system activates cleaning when power output decreases by 50%. The results highlight the effectiveness of this mechanism in maintaining solar panel performance, even in dusty conditions.

This study (Jaszczur et al.,2019) conducted in Kraków, Poland, focuses on evaluating the efficiency degradation of polycrystalline photovoltaic modules due to natural dust deposition, especially in an area with high pollution and low wind speed. The research

findings revealed that the efficiency loss due to deposited dust gradually increases with the mass and follows an exponential trend. The maximum observed dust deposition density led to about a 2.1% efficiency loss. This efficiency loss not only depends on the dust mass but also on dust properties. The study provides a reliable model for estimating PV module efficiency degradation caused by dust deposition, with a novel approach that is easy to apply and applicable to various geographical regions. This model is valuable for system designers and computer modeling in both urban and non-urban polluted areas.

This laboratory study (Adigüzel et al.,2019) examines the impact of coal dust, varying in size and weight, on the performance of photovoltaic (PV) modules. Monocrystalline silicon (m-Si) and polycrystalline silicon (p-Si) PV modules were tested under Standard Test Conditions, with coal dust particles categorized into six groups based on size. Artificial pollution was created by uniformly distributing coal dust of different sizes and weights on PV modules, with three weight levels (5g, 10g, and 15g) for each size of coal dust. The study measured voltage, current, and power to assess PV module performance and used this data to develop an Adaptive Neuro-Fuzzy Inference System (ANFIS) model. The comparison between experimental and ANFIS results indicated high accuracy with low Root Mean Square Error (RMSE) and a high coefficient of determination (R^2). For m-Si PV modules, RMSE was 0.18719, and R^2 was 0.99803, while for p-Si PV modules, RMSE was 0.87098, and R^2 was 0.99714. This demonstrates the success of the ANFIS model in estimating power for PV modules with specific particle sizes and weights.

This study (Styszko et al.,2019) investigates the impact of solid particles on the performance of photovoltaic (PV) modules, leading to power losses, reduced efficiency, increased temperature, and decreased lifetime. The study focuses on dust deposition on the PV front cover glass during the non-heating season in Kraków, one of Europe's most polluted cities. It analyzes the time-dependent particle deposition and its correlation with air pollution, particularly particulate matter. The research collected dust on PV modules exposed for varying durations (from 1 day to 1 week) and also gathered samples of total suspended particles (TSP) on quartz fiber filters. The findings reveal that dust deposition density on the PV surface ranged from 7.5 to 42.1 mg/m² for 1-day exposures, while weekly deposition densities ranged from 25.8 to

277.0 mg/m². Precipitation volume, intensity, and humidity significantly affect dust accumulation, with an estimated dust accumulation rate of around 40 mg/m²/day during non-precipitation periods, potentially influenced by electrostatic forces.

This paper (Cipriani et al.,2020) presents an innovative method for categorizing losses in photovoltaic (PV) systems using thermographic non-destructive tests (TNDTs) along with artificial intelligence techniques. Low electricity production in PV systems often results from decreased efficiency in PV modules due to abnormal operating conditions, such as failures or malfunctions. Among these conditions, dirt accumulation on the module surface is common, and its impact varies based on several factors. TNDTs are employed to identify these issues. The proposed method employs a convolutional neural network (CNN) to automatically classify thermographic images and achieves a 98% accuracy rate within a few minutes. Compared to existing approaches, this method offers advantages including faster execution, diagnosis speed, reduced costs, and minimized electricity production losses.

In (Saquib et al., 2020), the current market offers solar panels with efficiency ratings ranging from 15% to 22.8%, although the theoretical maximum efficiency can reach 86.6%. However, real-world conditions and factors such as dust significantly impact the performance of terrestrial solar panels. In the UAE region, dust accumulation is a common issue, and this paper utilizes image processing to detect dust levels. The percentage of dust is integrated into neural networks, alongside irradiance data, to predict the panel's voltage. When the voltage drops below a specific threshold, a cleaning signal is activated to maintain optimal performance.

This paper (Abuqaaud&Ferrah,2020) introduces a computer vision-based method designed to identify and assess soil and dust accumulation on photovoltaic panels. The experimental results of this study indicate that the proposed system achieves high recognition rates. The innovative approach offers a practical and straightforward solution that can lead to a more efficient and automated cleaning process for photovoltaic panels.

In (Maity et al .,2020), The growing number of solar farms faces challenges related to maintenance and operation. Environmental factors, particularly dust accumulation on solar panels, significantly impede power generation. This paper highlights a CNN-based approach for detecting dust on solar panels and predicts the resulting power loss.

The study involves capturing RGB images of solar panels in an experimental setup to estimate the impact of dust accumulation on power generation.

This study (Masoom et al., 2021) investigates the impact of dust on solar irradiance and energy forecasting during an extreme dust event. It combines various data sources including Aero net measurements, satellite observations, dust databases, and weather models. The research focuses on the northwestern part of the Indian subcontinent, an area with significant solar power projects. The study reveals that severe dust storms in May 2018 resulted in a substantial reduction in solar irradiance, affecting energy production from photovoltaic and concentrating solar power systems. The proposed methodology can assist in optimizing energy production forecasting and system maintenance, considering the impact of dust aerosols.

Dust accumulation on PV panels causes energy loss. Various techniques, including thermal imaging, image processing, sensors, cameras, machine learning, and deep learning, are being explored for dust detection. This study introduces a dataset of dusty and clean panel images and applies it to state-of-the-art classification algorithms. Additionally, a new CNN architecture, SolNet, is proposed for dust detection, achieving a high accuracy of 98.2%. The dataset and SolNet can serve as benchmarks for future research and can be expanded for multiclass classification with SolNet fine-tuning for further improvements (Onim et al.,2022).

This paper (Fan et al .,2022) introduces a novel image enhancement algorithm for assessing dust accumulation on photovoltaic (PV) panels. It utilizes an atmospheric scattering model to differentiate between clean and dusty PV panels based on image characteristics. The algorithm establishes a relationship between model coefficients and dust levels, achieving 83.78% accuracy. The average root mean square error (RMSE) for samples 1-4 is 1.67, and the error range is 2-3.5 g/m². Compared to optical attenuation and weighing methods, this approach offers higher accuracy with a mean absolute error (MAE) of 1.61 g/m². It provides a simple and reliable method for intelligent PV panel cleaning.

This paper (Fan et al.,2022) presents a novel method for quantitatively analyzing uneven dust accumulation on photovoltaic (PV) panels. It employs a deep residual neural network (DRNN) to assess regional dust concentration, enhancing prediction accuracy. An image preprocessing method is designed for dust accumulation

classification. The DRNN achieves an R2 of 78.7% and a mean absolute error (MAE) of 3.67. The method demonstrates consistency with error loop coefficients of 1.19, 0.77, and 1.10 under three different conditions. This approach provides theoretical support for intelligent PV system operation and maintenance.

To promote the deployment of photovoltaic (PV) systems for green energy goals, addressing dust accumulation on PV panels is crucial, especially in desert regions. This paper introduces an intelligent system for dust level detection on PV panels to optimize cleaning units. Unlike prior methods, it utilizes data on solar irradiation, power generation, and forecasted temperature. An expert artificial intelligence (AI) system on MATLAB processes and predicts data, enhancing accuracy. This approach is tested with real-world data under various weather conditions, demonstrating its feasibility (lfaris,2023).

This study (Cruz-Rojas et al., 2023) explores three distinct approaches that leverage semantic segmentation to tackle this problem. The first approach adopts unsupervised learning techniques, while the second employs supervised learning, utilizing a range of Machine Learning methods including K-means, Gaussian Mixture Models, Random Forest, Light GBM, as well as simpler options like histogram segmentation and color space analysis. The third approach harnesses Deep Learning models, with a focus on different variations of the U-net architecture, originally designed for image segmentation tasks. The study evaluates these approaches based on parameters like accuracy, processing time, training time, F1 Score, and Intersection over Union.

CHAPTER THREE
BACKGROUND THEORIES

3.1 Introduction

In this chapter, the main concepts of the methods used in this framework are presented and elaborated. The main issues includes image preprocessing, feature extraction methods, classification approaches, model performance metrics, and models evaluations.

3.2 Image File Formats

The image file format is a method for arranging and storing images on devices such as computers, tablets, and smartphones. The most common formats are JPEG, TIF, GIF, and PNG.

Joint Photographic Experts Group (JPEG) format is a common file formatting widely used on the internet, and JPEG is a popular digital camera format, making it excellent for web use and non-professional prints. JPEG file is a lossy format that means there is a quality reduction because of the compression, but it is usually not noticeable. Tag Image File Format (TIFF) files are lossless compression, which means they don't have to compress or lose any image quality or information that provides very high-quality photos with large file sizes. TIFF format is widely used in the graphics field, because of the graphic and printing quality that provides. Graphics Interchange Format (GIF) files are commonly used in web graphics because they are limited to only 256 colors. GIF files are based on the LZW (Lempel–Ziv–Welch) compression process, which is a data compression without loss of quality. GIFs have a size typically less than JPEG. Portable Network Graphics (PNG) files format is a lossless image format that was made to improve on the GIF format. PNG files can hold up to 16 million colors, Unlike GIF, which only supports 256 colors. PNG files are modern format, a little smaller than GIF and TIFF formats, and a good choice for lossless quality work (Qasim&Alyousuf,2021).

3.3 Real-time software applications

Real-time software applications are prevalent these days because they allow computers to handle jobs, activities, and operations more quickly. A realtime application often enables the user to execute many tasks and activities while the program is operating. Real-time systems in computers, on the other hand, enable numerous applications to run continuously, even if the user is only using one application or program. Some of these apps are considered system tasks in a computer system, built expressly to accomplish specified duties, reacting to the computer's time clock and providing results even if they are not launched by the user. Real-time systems are ones whose accuracy is dictated by the time it takes to create the result, including the final result of computation (Gupta et al.,2013;Laplante,2004).

3.4 Computer Vision

Computer vision is a subfield of computer science and artificial intelligence that uses machine learning and deep learning methods allowing computers to analyze, apply image processing methods, and automatically extract information from images or videos. Computer vision has an important role in many fields such as healthcare and medicine, sports, agriculture and farming, transportation, retail, and manufacturing. Computer vision was used in image classification, object detection, object tracking, and segmentation (Klein et al.,2012;Lampert&Lampert,2009).

3.5 Machine learning

Machine learning is a branch of computer science and artificial intelligence (AI) that offers systems that can learn and train from experience or collect data without being directly programmed and enhance their performance over time. There are three categories of machine learning algorithms supervised learning, unsupervised learning, and reinforcement learning. Machine learning uses the statistics theory in building mathematical Models, to solve the optimization problem an efficient algorithm must be chosen by taking several parameters into concern such as memory size, parameterization, overfitting, and time of training (Solem,2012). The main benefit of using machine learning is that if an algorithm knows what to do with input, it will automatically do its job and generate the outcome (Bonaccorso, 2017).

3.5.1 Supervised learning

Models are trained to generate the desired output using supervised learning, which uses a training dataset. This training dataset contains inputs and correct output that allow the model to learn over time. To calculate the algorithm's accuracy loss function is used, and it is modified until the error has been reduced to an acceptable level. Classification and regression are the subclasses of supervised learning (Dey,2016). Classification is an algorithm used for re-creating class assignments, in which the output value is discrete. When the classification output two values 0 or 1 then it is called binary classification, and when the classification output is more than two values then it is called multi-class classification. The most popular classification algorithms are support vector machines (SVM), Linear classifiers, k-nearest neighbor, decision trees, and random forest (Ayodele,2010). Regression is a predictive statistical technique in which the model tries to find a relationship between the dependent and independent variables. A regression algorithm aims to estimate a continuous output closed to the real evaluation, like test score, and sales. Linear regression, logistic regression, and polynomial regression are the common types of regression algorithms (Sen et al., 2020).

3.5.2 Unsupervised learning

Unsupervised learning is a machine learning method that does not use labeled datasets to organize models. The model itself discovers hidden patterns and observations in the results. It is equivalent to the learning that happens in the human brain when learning new things. Because it includes input data but no corresponding output, unsupervised learning cannot be used directly to regression or classification problems like supervised learning. Unsupervised learning tries to reveal a dataset's underlying structure, categorize data based on similarities, and show it in a compressed format. The common types of unsupervised learning techniques are, clustering, and association problems. The popular algorithms of unsupervised learning are K-means clustering, and Hierarchal clustering (Bengio et al.,2017). Clustering is a method of categorizing items so that those with the most similarities stay in one category while those with fewer or no similarities stay in another. Cluster analysis finds similarities among data objects and categorizes them based on whether those similarities exist or

not. An unsupervised learning method that discovers correlations between variables in a large database is known as an association. It detects the set of objects in the dataset that appear together. The association rule increases the efficiency of marketing campaigns (Olaode et al.,2014).

3.5.3 Reinforcement Learning

Reinforcement learning is a branch of machine learning in which a combination of action and a specific state of the environment is used to determine the probability of earning a certain amount of reward as well as how the state will change. The objective of reinforcement learning is to find the best strategy or behavior for each state that maximizes the expected value of potential rewards. Reinforcement learning is especially effective when the environment is not entirely deterministic, when it is often very dynamic, and when precise error measurement is impossible (Solem,2012).

3.6 Deep Learning

Deep Learning is a part of machine learning that simulates the structure and function of the human brain using artificial neural networks. Deep learning is identified as deep structured learning or hierarchical learning that extract features from data and use a large number of hidden layers and converts them into several levels of abstraction. When dealing with unstructured data, deep learning achieves higher power and flexibility by processing many features. The data is passed through multiple layers of the deep learning algorithm, each of which can extract features and move them on to the next layer. The first layer extracts low-level features, then they combined with subsequent layers to form a complete representation. Recurrent neural networks (RNN), artificial neural networks (ANN), convolutional neural networks (CNN), and other types of deep learning neural networks are transforming how we interact with the world. There are many applications of deep learning like self-driving cars, unmanned aerial vehicles, and speech recognition. The deep learning structure is shown in Figure (1) (Hodeghatta & Nayak, 2017;Mathew et al.,2020).

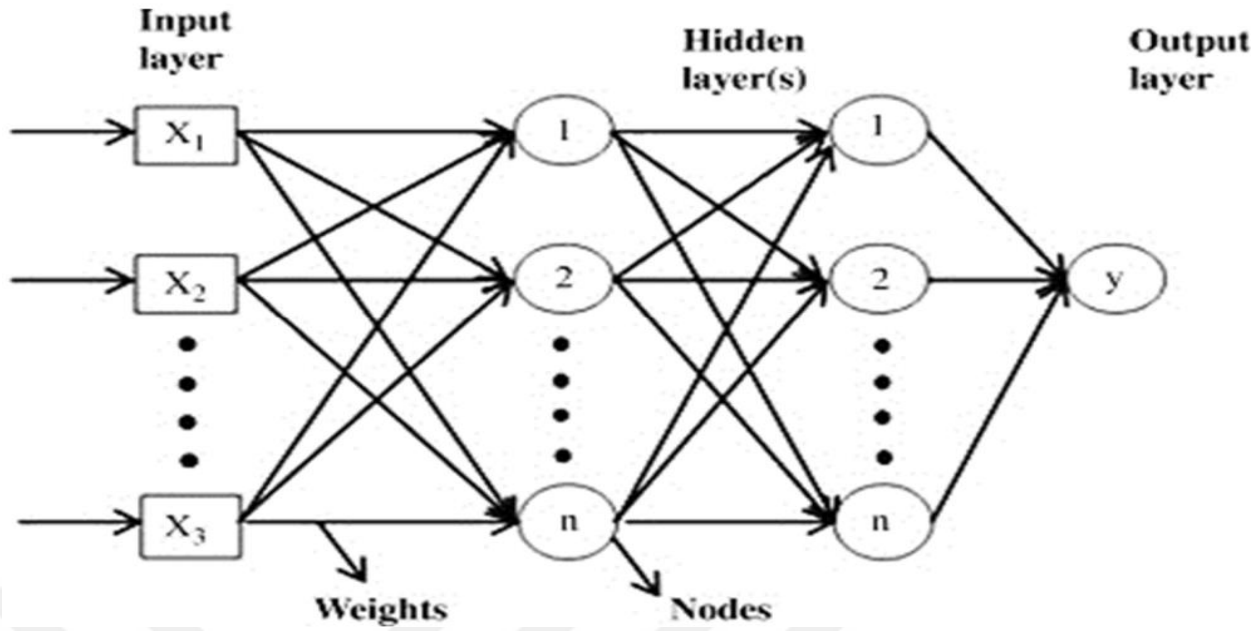

Figure 14. Deep Learning Network (Mathew et al., 2020).

3.6.1 Convolution Neural Network (CNN)

A common type of deep learning algorithms is CNN that consists of multiple artificial neural layers. CNN takes input data then assigns significant learnable weights, and biases to detect various features, and distinguish between them. CNN algorithm is a forward neural network and it is considerably better than classical neural networks because it can train smoothly due to the less number of features parameters that need, and the high efficiency of detecting features. Popular applications of CNN are image classification, objects detection, speech recognition, and facial recognition (Zaccone et al., 2017). The convolutional layer, pooling layer, and fully connected layer are the main layers of the CNN algorithm as shown in Figure (2). There are various models of CNNs such as MobileNet, GoogleNet, AlexNet, ResNet, SqueezeNet, VGG, and Inception (Indolia et al., 2018;Khan et al.,2020).

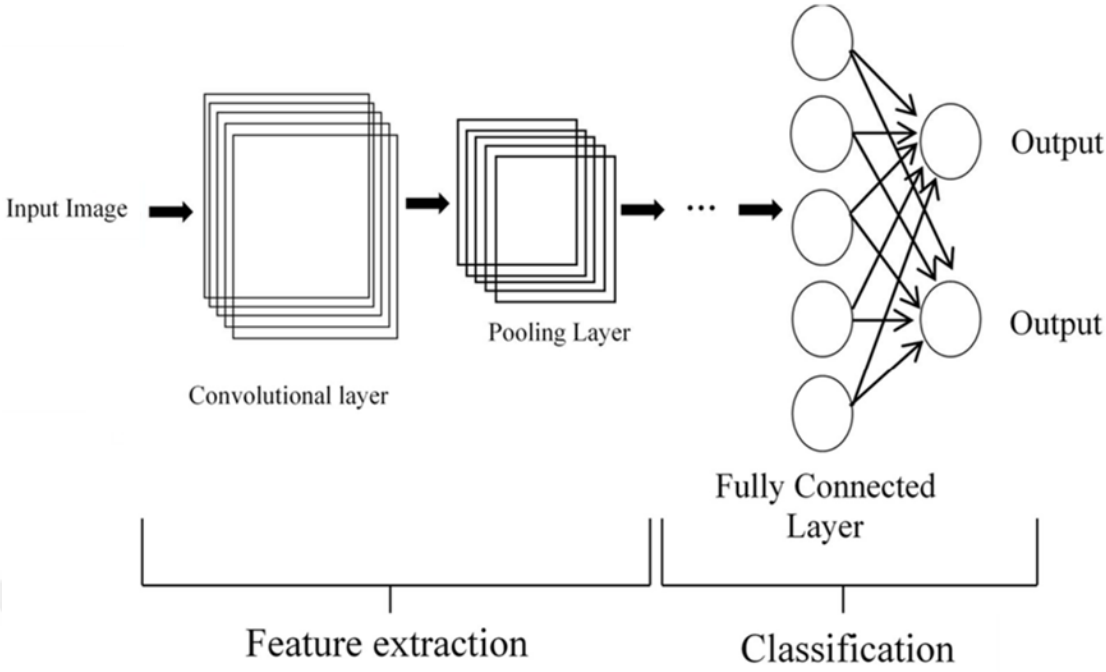

Figure 15. Convolution Neural Network Main Structure

3.6.1.1 Convolutional layer

The first layer of the CNN algorithm is the convolutional layer, in which various information is extracted from the input images. This layer performs the convolution mathematical process between the input image and a kernel filter of a specific size (M×M). Sliding the filter across the input image produces the dot product between the filter and the parts of the input image concerning the filter's size (M×M). The output of the convolutional layer is a feature map, which contains information about the image's corners and edges. Other layers use this feature map to learn a lot more features from the input image. After each convolutional layer an activation function was applied, in which the output of the layer converts it into some form that can be taken as input to the next layer. Rectified linear unit (ReLU), tanh, and sigmoid are types of activation functions, ReLU is the most non-linear effective function and its computational is easy as compared with other functions (Indolia et al.,2018). Convolutional layer operation is shown in Figure (3).

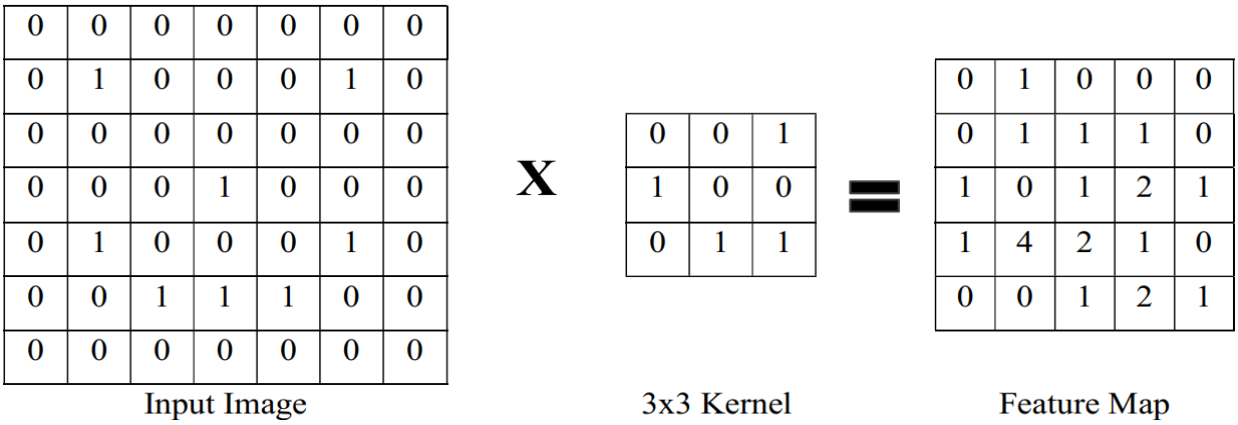

Figure 16. Convolutional Layer Operation (Indolia et al., 2018)

3.6.1.2 Pooling layer

A new layer called the pooling layer was added after the convolutional neural network to reduce the dimension of the feature maps. The amount of computation in the network and the number of parameters to learn are decreased. The pooling layer summarizes the features contained in a region of the feature map formed by a convolution layer. As a result, rather than the convolution layer's precisely positioned features, subsequent steps must be completed on summarized features. Hence the model will become more robust to the changes in feature position in the input picture. Average pooling and max pooling are the most popular types of pooling methods. Max pooling chooses the highest value from the feature map region covered by the filter. Consequently, the output of the max-pooling layer will be a feature map that contains the most important feature of the previous feature map. Average pooling is used to calculate the average of the elements present in the feature map covered by the filter. As a result, max-pooling identifies the most important features in a feature map patch, average pooling identifies the average of all features in that patch as shown in Figure (4) (Sinha&Hwang,2019).

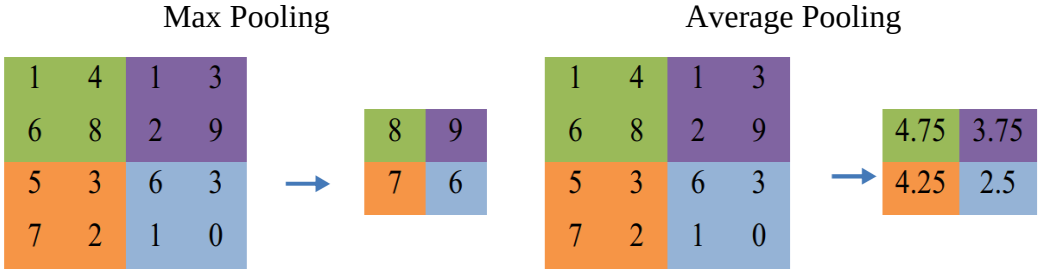

Figure 17. Max Pooling and Average Pooling Operator

3.6.1.3 Fully connected layer

The fully connected layer is a feed-forward neural network that is usually used for classification at the end of the network. The output of the pooling and convolutional layers is compressed and fed into the fully connected layer as a vector. By looking at the features of the training set, the fully connected layer is used to define the input image (Gholamalinezhad&Khosravi,2020).

2.6.2 MobileNetV2 model

Google released the MobileNets family of neural network architectures to be utilized on computers with limited computing power, such as mobile smartphones. MobileNets have high accuracy with low power and memory consumption making them the fastest networks family to be used in image processing. MobileNet is based on depth wise separable convolutions, which divide a standard convolution into a depth wise convolution that applies a single filter to each input channel and a 1 × 1 convolution known as a pointwise convolution, whereas standard convolution filters and combines inputs in one step to create a new set of outputs, as shown in Figure (5). This factorization decreases computation time and model size as seen in Equations (3-1, 2, 3) (Albawi et al., 2017)he computational cost of standard convolutions is:

$$Computational\ cost = D_k.D_k.M.N.D_F.D_F \quad (3.1)$$

The cost of depth wise separable convolution is:

$$Computational\ cost = D_k.D_k.M.D_F.D_F + M.N.D_F.D_F \quad (3.2)$$

Where Dk × Dk is the kernel size, N is the number of output channels, *M* is the number of input channels, and DF × DF is the feature map size. We get almost 8 times less computational reduction when using depth wise separable convolution as in equation:

$$\frac{D_k.D_k.M.D_F.D_F+M.N.D_F.D_F}{D_k.D_k.M.N.D_F.D_F} \ \&\ Compution\ Reduction = \frac{1}{N} + \frac{M.N.D_F.D_F}{D_k.D_k} \quad (3.3)$$

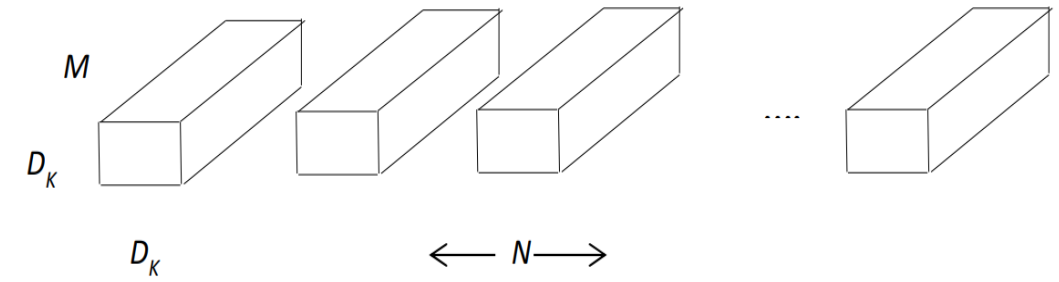

(a) Standard Convolution

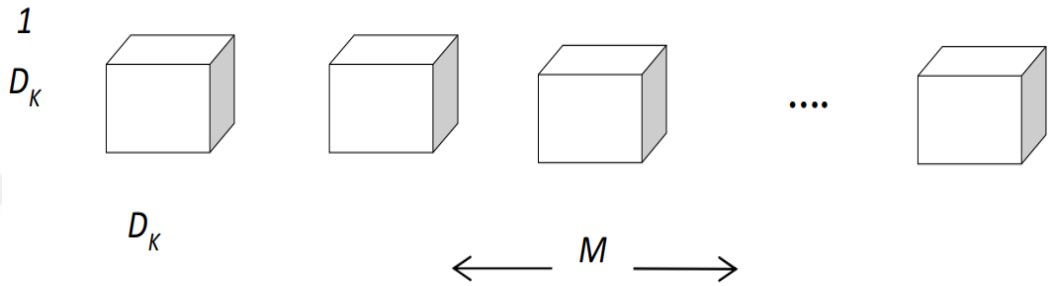

(b) Depth wise Convolutional Filters

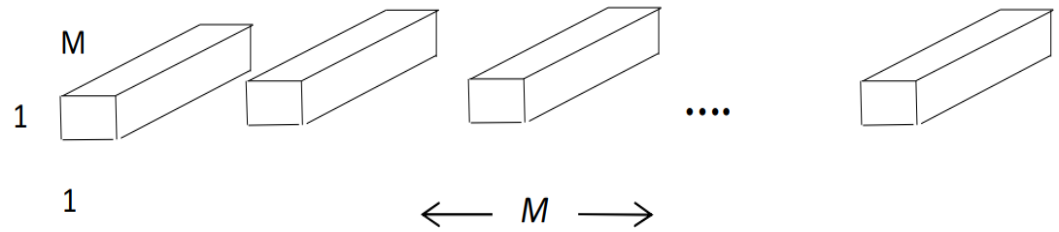

(c) 1x1 Pointwise Convolution Filters

Figure 18. Comparision between (a) Standard convolution, (b) Depth wise convolution, and (c) Pointwise convolution filters (Albawi et al.,2017)

MobileNet V2 architecture shown in Figures (6)(a) and (6)(b), contains 17 bottleneck residual blocks in a row then followed by a regular 1×1 convolution, a global average pooling layer, and a classification layer.

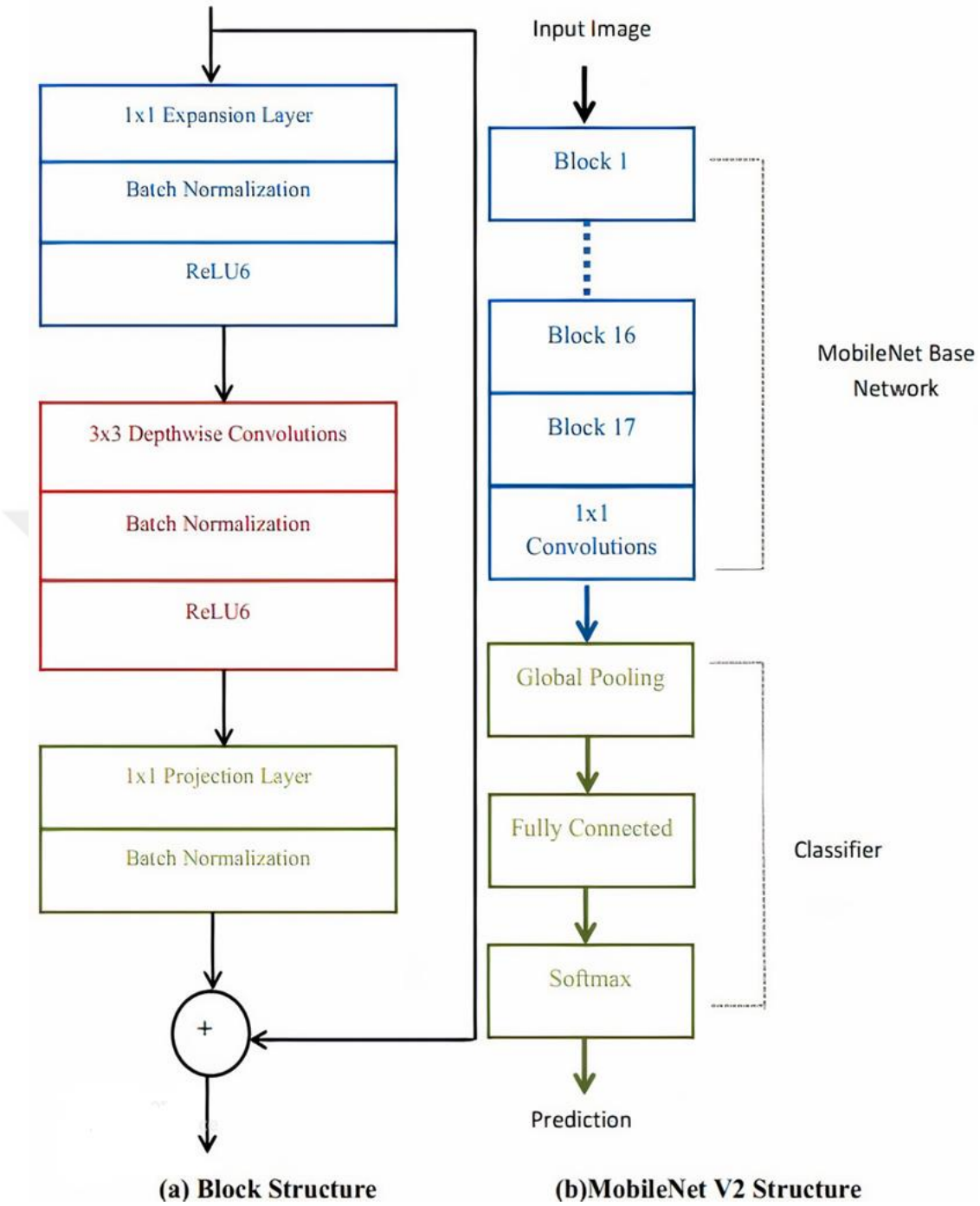

Figure 19. (a) Bottleneck Residual Block Structure (b) MobileNet Version 2 Structure (Howard et al.,2017)

There are three layers for each block, the expansion layer is the first layer used to increase the number of channels before entered to the next layer by multiplying the number of channels with a hyperparameter (expansion factor) followed by a batch normalization and ReLU a nonlinearity activation function, the second layer consist of

a depth wise convolution that filters the inputs also followed by batch normalization and RelU activation function, the last layer in the block have a pointwise convolution layer named a projection layer because it reduces the number of channels followed by a batch normalization (Nguyen,2020;Sandler et al.,2018).

3.7 Image Processing and CNN types

Image processing is a form of signal processing where the input is an image, such as a photograph or video frame, and the output is an image or a set of features that are elated to the input image. It's a technique used for performing certain operations on an image, such as enhancing it or extracting significant information from it. Analog and digital image processing are the two methods of image processing. Analog Image Processing (AIP) is a time-consuming and expensive method that works with an electrical wave and two dimensions analog signals like television images, photographs, and painting. Images are modified by altering the electrical signal in this form of processing. Digital Image Processing (DIP) is the other type of image processing that deals with digital images in which the image is represented by a matrix or array of pixels that have numerical values, these pixels are represented in the spatial domain. Digital image processing is easy, fast, and a cheap technique used to manipulate digital images by using digital devices like computers and digital phones. Image restoration, image analysis, image enhancement, and image compression, etc. are various types of image processing techniques (Sumithra et al.,2015). The fundamental purpose of image enhancement is to improve the appearance of a given image so that it is better suited for a particular application. It emphasizes or sharpens image features such as edges, boundaries, or contrast to improve the usability of a graphic display for presentation and analysis. The enhancement does not increase the data's inherent information content, but it does increase the dynamic range of the feature selection, allowing them to be identified more easily (Irmak&Ertas,2016).

3.7.1 Histogram Equalization

An effective image enhancing technique is histogram equalization that is used to improve image contrast by adjusting pixels intensities values to a uniform distribution and increasing the dynamic range of the image. There are three steps to histogram

equalization, in the first step the histogram of the image is determined, and then determine the normalized sum of the histogram in the second step, in the last step the transformation is calculated to transfer the old intensity values to new intensity values (Khehra&Devgun, 2015)**.**

3.7.2 Multitask Cascaded CNN (MTCNN) Algorithm

The MTCNN method is a deep convolutional neural network-based face identification and alignment technique that can detect and align faces simultaneously. MTCNN outperforms the traditional technique in terms of accuracy, speed, and ability to reliably locate the face; additionally, MTCNN can detect in real-time. MTCNN algorithm has three neural networks P-Net, R-Net, and O-Net. The original image should be scaled to several scales to construct an image pyramid before using these networks to achieve face recognition on a unified scale. In the first step, the proposed method has a 12 × 12 stage 1 kernel for each scaled copy that will scan the entire image for faces then it passed to P-Net to return the coordinates of a bounding box if the face was detected. The bound boxes with low confidence were deleted, the bound box coordinates were converted to unscaled image coordinates, Non-Maximum Suppression was used to reduce the number of overlapped bounding boxes, and the bound boxes were reshaped to square. In the second step bound boxes will padding this process was useful when the entire of the bond box is part of the face then its feds to R-Net. The same processes apply to the bound boxes in P-Net will be applied to bound boxes in R-Net. In last step the bound boxes will padding and enter to O-Net. The outputs of O-Net are the bond boxes coordinates, facial landmark coordinates, and the confidence level of each box. The low confidence bound boxes deleted, the coordinates of bounding boxes and facial landmark convert to un-scaled image coordinates, and non-Maximum suppression applied to all bound boxes. The output must be one bound box for each face in the image (Sontakke&Kulkarni,2015). Figure (7)(a), (7)(b), and (6)(c) depicted P-Net, R-Net, and O-Net structure respectively.

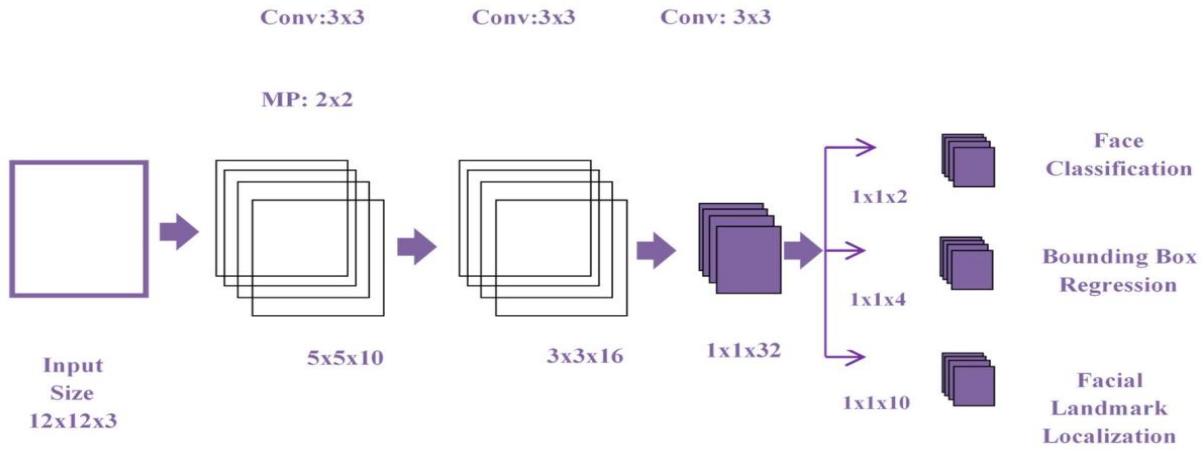

(a) P- Net

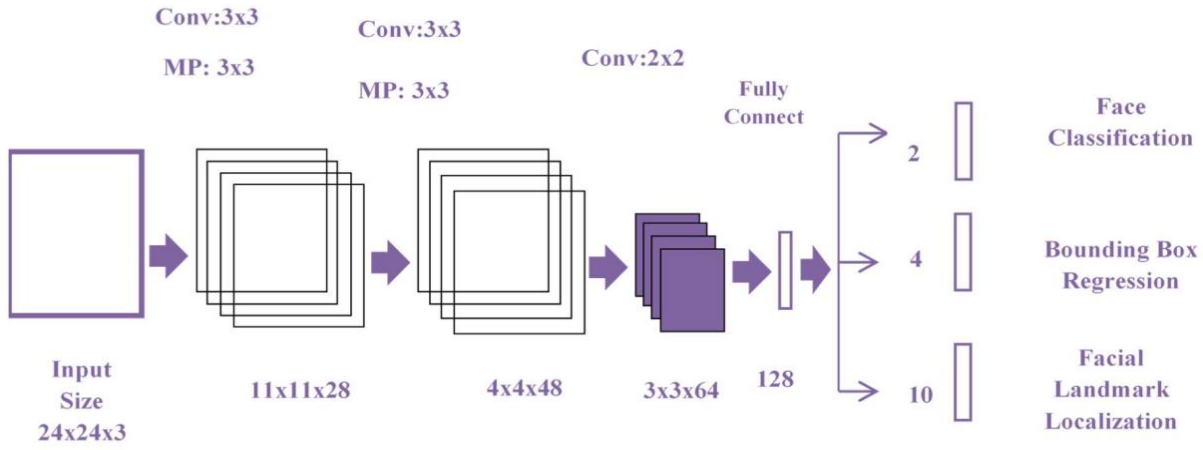

(b) R-Net

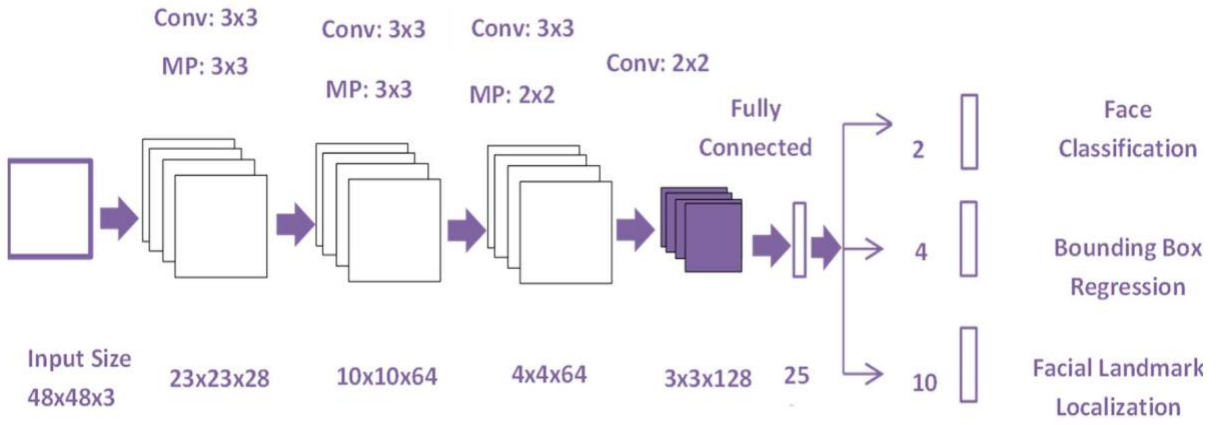

(c) O-Net

Figure 20. MTCNN Network Structure (Sontakke&Kulkarni,2015)

3.7.3 Filtering (Noise Reduction)

Noise reduction is a pre-processing technique that improves the outcomes of subsequent processing. Different Filters used to remove different types of noise from the image; filter selection is based on the type and amount of noise present in an image. Mean filter applies a mask to each pixel in the image and determines the average value of the corrupted image in a predetermined area, and then replaced the intensity value of the center pixel with this value. Mean filter is a linear filter the disadvantage of this filter that blurs the edges and destroys the fine details of an image (Hambal et al., 2017).

In digital image processing, median filtering is very common because it works well in some situations. The median filter is a non-linear filter used for reducing various types of noise. Median filtering is achieved by finding the median value surrounding the window and then replacing each entry in the window with the pixel's median value. The median is simple to calculate if the window has an odd number of entries. After all of the entries have been numerically sorted, it's the middle value. However, there are many medians for an even number of entries (Luo et al.,2020).

3.8 Data Acquisition and Camera Model

In this phase, these images were captured using a mobile camera which was used to record images or videos of the solar cells. The smartphone camera was fixed in different locations, this will ensure that the trained classification model will not be limited to a certain location or specific pose.

3.9 Dataset Preparation

Dataset preparation is a vital step in the development of an image dataset to ensure that the collected images are both suitable and error free before training. The recorded videos were captured using four different types of mobile cameras, mounted on different locations using a car phone holder to include any car vibrations and changing external lighting conditions. This diversity will ensure that training the detection model will include all types of external noise that may occur while driving, this will enhance that the trained classification model to be applicable for testing in real driving

conditions. The captured videos are then processed, and the individual frames are extracted.

3.10 Dataset Development

The total compiled dataset consists of 2562 images with size 224×224 collected from manually captured images of different subjects and different camera positions of PV panel images, the image distribution with nearly balanced as 1493 with no dust (clean) classified images and 1069 with dust (dusty) classified images. The dataset categorized into two classes namely clean, and dusty. During the training and validation processes 80% of images were used, where (2049 images) from the dataset were used for the training process and another (513 images) were used for validation and testing processes as 307 for validation and 206 for testing. The validation runs simultaneously with the training process to prevent model overfitting. For the testing process, we used some another 206 unlabeled images for the same subjects used for training the model, yet these images were never used neither in training nor the validation processes. The batch size for training is 16, so the epoch is 20 with 130 iteration each. The learning rate used is 0.001, while the momentum is 0.99.

3.11 Image Preprocessing

In this phase, firstly making data cleaning with eliminating duplicate, irrelevant images, or unlabeled images. The cleaned dataset is then loaded for the next preprocessing step (data augmentation) which are applied to the images before training to increase the detection ability of the model. The images rotated between - 90 and 90 degrees randomly that change the angles and direction of the images to increase the number of states that fed to the learning model, scaled images between 1 and 2 that doubled the size of some small images and remains the other images in random way, and reflected images randomly that flipped the images on the x and y axis. The nest process is to normalize all images by dividing on the max gray level and hence produce images with pixel values between (0-1). The last preprocessing step is to enhance the image using simple Gaussian and Laplacian filter. Figure (8) shows the data preprocessing steps that applied to the dataset. The prepared dataset is then splitted into training and testing parts to be passed to the training and validation process.

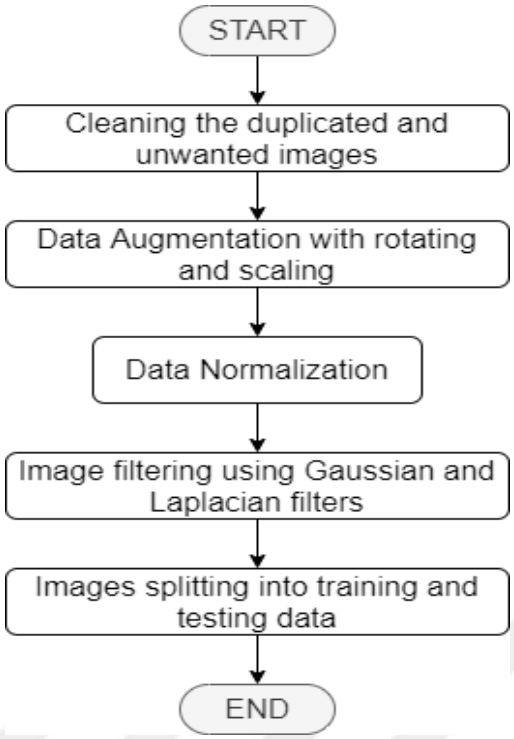

Figure 21. Data Preprocessing Steps Flowchart

3.12 Training the classification model

In the proposed models the convolutional neural network architecture with different structures were used due to its fast performance with faster processing time and low latency when compared with other deep learning models, shown in Table (1).

Table 1. Comparison and Benchmarking of AI Models and Frameworks on Mobile Device (Beauxis- Aussalet & Hardman,2014)

Model	**FLOPs (Millions)**	**Parameters (Millions)**
InceptionV3	5000	23.2
VGG-16	2800	8
ResNet50	3800	25.6
MobileNetV2	300	3.4

The proposed models in this study leverage convolutional neural network (CNN) architecture, chosen for its notable advantages in terms of fast performance, quicker processing times, and low latency. CNNs are particularly well-suited for image-related

tasks, making them a popular choice for applications involving visual data. It can make simple comparison:

- **Computational Efficiency:**

- MobileNetV2 stands out as the most computationally efficient among the models, making it ideal for deployment on mobile devices with limited resources.

- VGG-16, despite its simplicity, shows competitive performance with moderate computational requirements.

- InceptionV3 and ResNet50 exhibit higher computational loads, potentially limiting their deployment on resource-constrained devices.

- **Model Complexity:**

- InceptionV3 is known for its intricate architecture, allowing it to capture complex patterns in data.

- VGG-16 maintains a simpler architecture but is still effective in various computer vision tasks.

- ResNet50 introduces residual connections, addressing training issues in deeper networks.

- MobileNetV2 is optimized for simplicity and efficiency, sacrificing some complexity for resource savings.

- **Parameters:**

- In terms of parameter count, VGG-16 has the lowest, making it a more lightweight model in comparison.

- MobileNetV2 has the fewest parameters, indicating a streamlined design for mobile deployment.

- InceptionV3 and ResNet50 have higher parameter counts, offering more capacity for learning intricate features.

We take the initialize learning rate 0.001, momentum rate 0.99, minimum batch size 16, and the hardware resources is single GPU (Nvidia with 4 GB). All models were need to modify to be able for binary classification (clean, and dusty). The last four layers were replaced by batch normalization layer, dense layer, dropout layer, and the last dense layer. After training the classification model, we test the performance of the

model with the testing set of images and with the external testing set as seen in Figure (9).

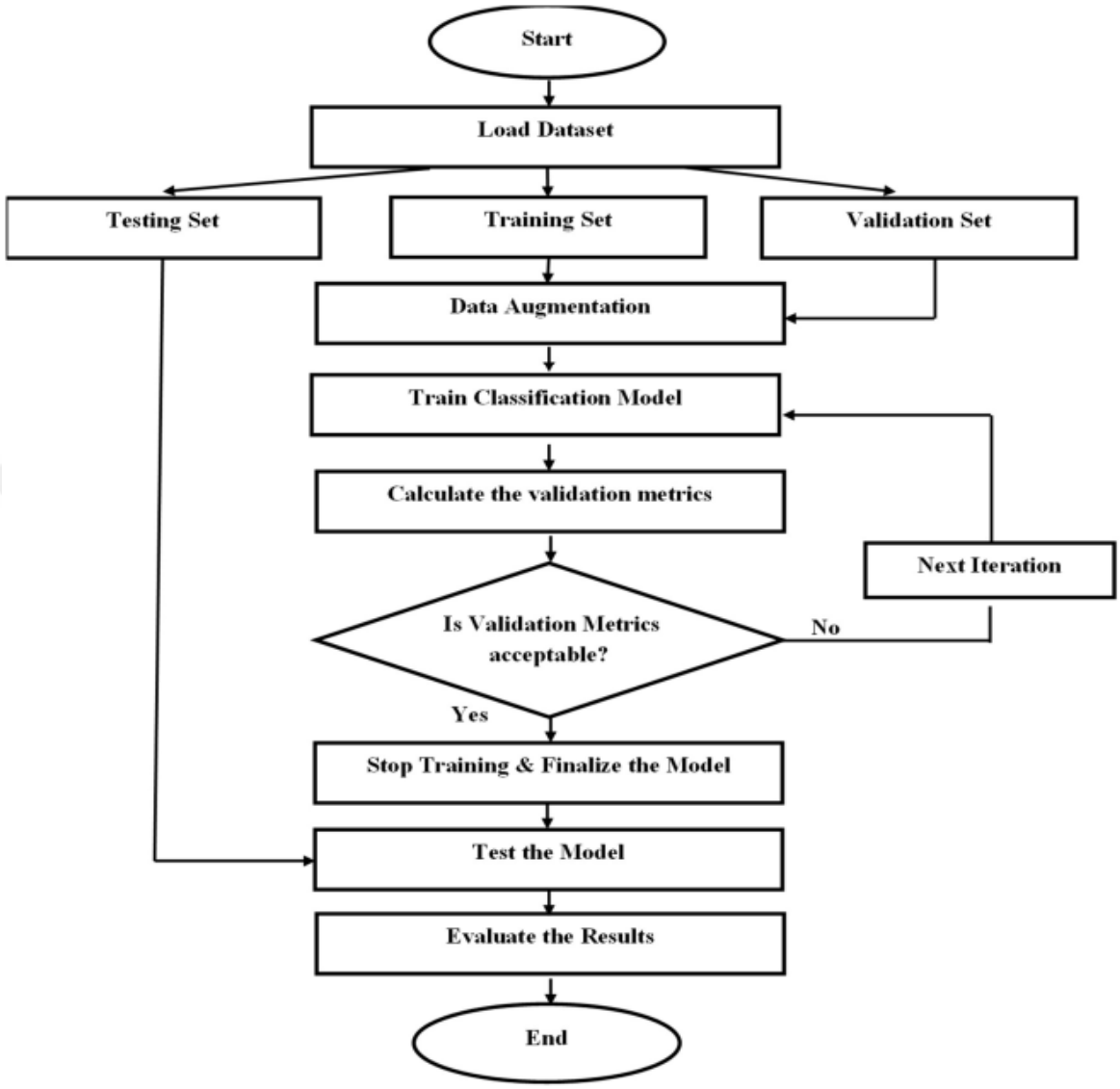

Figure 22. Flowchart of dataset distribution that used for training and testing the proposed model

3.12.1 Inception v3

Inception v3 is a convolutional neural network (CNN) architecture designed for image classification tasks, particularly within the field of computer vision. It is part of the Inception family of models developed by Google's research team. The primary goal of

Inception v3 is to enhance both accuracy and efficiency in image recognition tasks compared to its predecessors.

Key features and components of the Inception v3 model as shown in Figure (10) include:

1. Structure:

- Inception v3 follows a deep neural network architecture with multiple layers of convolutional and pooling operations. It is characterized by its unique "Inception" modules, which incorporate parallel convolutional operations of different filter sizes within the same layer.

2. Inception Modules:

- Inception modules are fundamental building blocks in the Inception v3 architecture. These modules consist of multiple parallel convolutional and pooling operations, allowing the network to capture features at various scales and resolutions simultaneously.

3. Factorization:

- Inception v3 employs factorization to reduce the computational cost of convolutions. This involves breaking down large convolutions into smaller, more manageable convolutions, which helps improve efficiency without sacrificing performance.

4. Batch Normalization:

- Batch normalization is utilized to improve the stability and convergence of the model during training. It normalizes the input to a layer, mitigating issues related to internal covariate shift and accelerating the training process.

5. Auxiliary Classifiers:

- Inception v3 introduces auxiliary classifiers at intermediate layers during training to combat the vanishing gradient problem. These auxiliary classifiers assist in providing additional supervision signals, aiding the model in learning useful representations.

6. Global Average Pooling:

- Instead of traditional fully connected layers towards the end of the network, Inception v3 utilizes global average pooling to reduce the spatial dimensions of the

feature maps. This contributes to a reduction in the number of parameters, minimizing overfitting and enhancing generalization.

7. Pre-trained Weights:

- Inception v3 is often pre-trained on large image datasets, such as ImageNet, to leverage learned features and weights. Transfer learning with pre-trained models allows Inception v3 to be adapted to specific tasks with smaller datasets more effectively.

8. Applications:

- Inception v3 is widely used for various computer vision applications, including image classification, object detection, and image segmentation. Its versatility and efficiency make it suitable for real-time and resource-constrained scenarios.

In summary, Inception v3 is a state-of-the-art deep learning model that leverages innovative architectural design, factorization, and auxiliary classifiers to achieve high accuracy in image classification tasks while maintaining computational efficiency. Its adaptability and pre-trained weights make it a valuable tool for a range of computer vision applications.

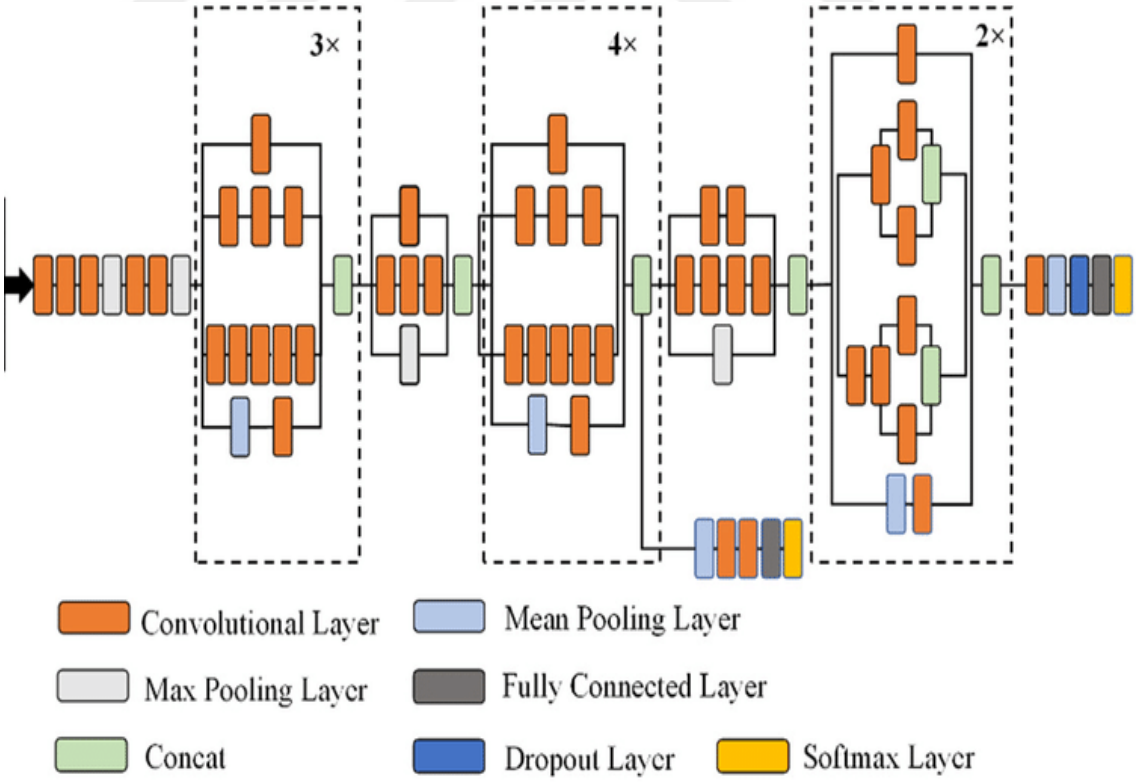

Figure 23. The architecture of Inception v3 model

3.12.2 VGG-16

VGG-16, short for the Visual Geometry Group 16-layer model, is a convolutional neural network (CNN) architecture that gained prominence for its straightforward yet effective design. Developed by the Visual Geometry Group at the University of Oxford, VGG-16 is known for its deep architecture with a focus on using small-sized convolutional filters consistently throughout the network. Here's a comprehensive description of the VGG-16 model as illustrated in Figure (11):

1. Structure:

- VGG-16 consists of 16 layers, including 13 convolutional layers and 3 fully connected layers. The convolutional layers are stacked with small receptive fields (3x3 filters) and use max-pooling layers to downsample the spatial dimensions.

2. Convolutional Layers:

- The convolutional layers in VGG-16 are characterized by the repetitive use of 3x3 convolutional filters. This design choice aims to maintain a small receptive field while deepening the network, allowing it to capture intricate features in the input images.

3. Pooling Layers:

- VGG-16 employs max-pooling layers after every two convolutional layers to reduce the spatial dimensions of the feature maps, progressively capturing more abstract and complex features as the network deepens.

4. Fully Connected Layers:

- The final layers of VGG-16 include three fully connected layers, followed by a softmax layer for classification. These layers combine high-level features learned by the convolutional layers to make predictions across different classes.

5. Activation Function:

- Rectified Linear Units (ReLU) serve as the activation function throughout the network, introducing non-linearity and aiding in the learning of complex representations.

6. Number of Filters:

- The number of filters in each convolutional layer gradually increases as the network deepens, allowing the model to learn hierarchical features of increasing complexity.

7. Pre-trained Models:

- VGG-16 is often pre-trained on large image datasets, such as ImageNet, leveraging learned features and weights for transfer learning on specific tasks. This pre-training helps the model generalize well to a wide range of visual recognition tasks.

8. Applications:

- VGG-16 has been successfully applied to image classification tasks, where its deep architecture and systematic design contribute to achieving state-of-the-art performance. It has also been used as a feature extractor in various computer vision applications, including object detection and image segmentation.

9. Drawbacks:

- While VGG-16 is effective, its deep architecture with a large number of parameters can lead to increased computational complexity and memory requirements, making it less suitable for real-time and resource-constrained applications compared to more recent architectures like ResNet or Inception.

In summary, VGG-16 is a widely recognized CNN architecture known for its simplicity and effectiveness in image classification tasks. Its systematic design with small convolutional filters and a deep structure contributes to its success in capturing intricate features in visual data. Pre-trained VGG-16 models serve as valuable tools for transfer learning in various computer vision applications.

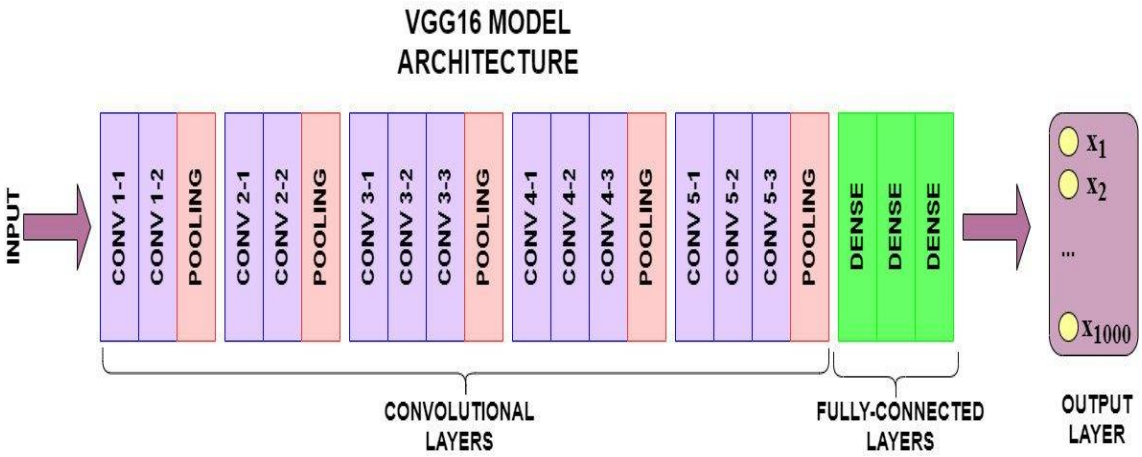

Figure 24. The architecture of VGG-16 model

3.12.3 Resnet-50

ResNet-50, short for Residual Network with 50 layers, is a convolutional neural network (CNN) architecture that introduced the concept of residual learning. Developed by researchers at Microsoft Research, ResNet-50 addresses the challenges associated with training very deep networks by utilizing residual blocks. Here's a comprehensive description of the ResNet-50 model as shown in Figure (12):

1. Residual Blocks:

- The core innovation in ResNet-50 is the introduction of residual blocks. These blocks contain shortcut connections that skip one or more layers, allowing the model to learn residual functions. This enables the network to effectively capture and propagate information through very deep architectures.

2. Deep Architecture:

- ResNet-50 is a deep neural network consisting of 50 layers, including both convolutional and fully connected layers. The deep architecture is made possible by the use of residual blocks, which alleviate the vanishing gradient problem associated with training deep networks.

3. Convolutional Layers:

- The convolutional layers in ResNet-50 use small 3×3 filters in combination with larger 1×1 filters. The use of smaller filters allows the network to capture spatial hierarchies effectively.

4. Identity Shortcuts:

- The identity shortcuts in the residual blocks enable the model to learn residual mappings, making it easier for the network to converge during training. These shortcuts also aid in the flow of information, mitigating the degradation problem observed in very deep networks.

5. Global Average Pooling:

- Instead of traditional fully connected layers towards the end of the network, ResNet-50 employs global average pooling. This technique helps reduce the spatial dimensions of the feature maps, minimizing the number of parameters and addressing overfitting.

6. Pre-trained Models:

- ResNet-50 is often pre-trained on large image datasets, such as ImageNet. This pre-training facilitates transfer learning, allowing the model to adapt its learned features to specific tasks with smaller datasets.

7. Skip Connections:

- The skip connections in ResNet-50 enable the gradient to flow more directly through the network during backpropagation, facilitating the training of very deep networks. This design choice enhances the ability of the model to capture complex features.

8. Applications:

- ResNet-50 is widely used for image classification tasks and has achieved state-of-the-art performance on various benchmark datasets. Its ability to effectively train very deep networks makes it suitable for a range of computer vision applications, including object detection, image segmentation, and facial recognition.

9. Drawbacks:

- While ResNet-50 is powerful, its deep architecture comes with increased computational complexity and memory requirements. This can limit its deployment in resource-constrained environments, and more lightweight architectures may be preferred for certain applications.

In summary, ResNet-50 is a groundbreaking CNN architecture that introduced residual learning to address the challenges of training very deep networks. Its use of residual blocks, identity shortcuts, and skip connections enables the effective training of deep models, making it a popular choice for various computer vision tasks.

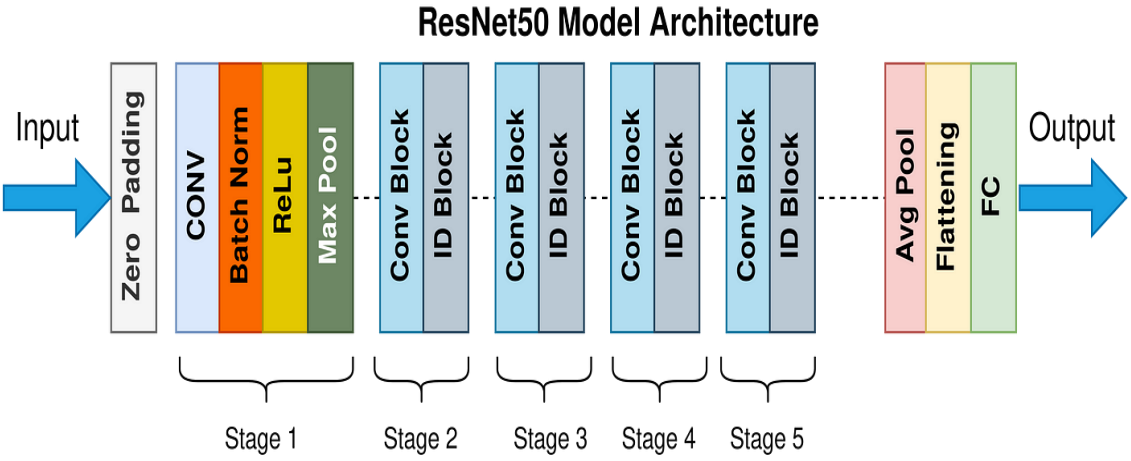

Figure 25. The architecture of ResNet-50 model

3.13 Model's Performance

In this work and to remove the noise from images, we applied a [5×5] median filter with Gaussian and Laplacian processes because its ability to remove different types of noise with efficient and simple way without distorted the image or remove the important details and information's from the image. Test accuracy of the model and the other metrics that used to evaluate the model was measured with normal captured images, noisy images, and denoising images after using median filter.

The performance of median filter is evaluated using four metrics which are the Accuracy, Recall, Precision, and F-score while the loss or the error is evaluated using mean square error (MSE).

To summarize the classification model performance confusion matrix was used; it's a matrix that can help us to calculate many metrics to evaluate the model by finding (TP, TN, FP, and FN). True positives (TP): Means that we predicted clean images. True negatives (TN): In which we predicted dusty images. False positives (FP): We predicted dusty, but they are clean. False negatives (FN): We predicted clean, but they are dusty. The confusion matrix, accuracy, recall, precision, and f1-score (the average of recall and precision) metrics as in as in Equations (3.4-3.7) (Irmak&Ertas,2016;Luo at el.,2020).

$$Accuracy = \frac{T_P+T_N}{T_P+T_N+F_P+F_N} \quad (3.4)$$

$$Recall = \frac{T_P}{T_P+F_N} \quad (3.5)$$

$$Precision = \frac{T_P}{T_P+F_P} \quad (3.6)$$

$$F-Score = \frac{2T_P}{2T_P+F_P+F_N} \quad (3.7)$$

The Mean Square Error (MSE) is defined as a sum of square of the error between two images. MSE can be calculated using the following equation (Beauxis-Aussalet& Hardman,2014):

$$MSE = \frac{1}{MN}\sum_{i=1}^{M}\sum_{j=1}^{N}(f(i,j)-g(i,j))^2 \quad (3.8)$$

Where, *M* and *N* are the dimensions of the image in pixels, *f(i,j)* is the noisy image and *g(i,j)* is the filtered image.

CHAPTER FOUR
EXPERIMENTIAL RESULTS

4.1 Introduction

In this chapter, the main concepts of the PV dust detection in deep learning methods used in this framework are presented and elaborated. The main issues includes image preprocessing, feature extraction methods, deep learning classification approaches, model performance metrics, and models evaluations. This comprises implementing different systems for accurately classifying local and global PV panel images with clean and dusty classes. These systems include CNN, RESNET, VGG-16, INCEPTION-3, and NETB0 deep learning architecture models. CNN is crucial and it is one of the major constraints to the actual application of suitable classifiers. The PV panel images dataset that are used to detect two types of classes were obtained from the locally and globally sites. Finally, performance metrics are evaluated to cover the testing and assessment for the suggested systems.

4.2 Dataset Acquisition and Preprocessing

The data collecting process is considered a fundamental stage in this study, since many images of the PV solar cells were acquitted by suitable imaging scans facility different PV places at the world. The dataset consists of 2562 colored images with size 224×224 collected from different camera positions of PV panel images. The distribution of these images is nearly balanced as 1493 with no dust (clean) classified images and 1069 with dust (dusty) classified images. Figure (1) shows a sample of this dataset images which are randomly selected from the clean and dusty groups.

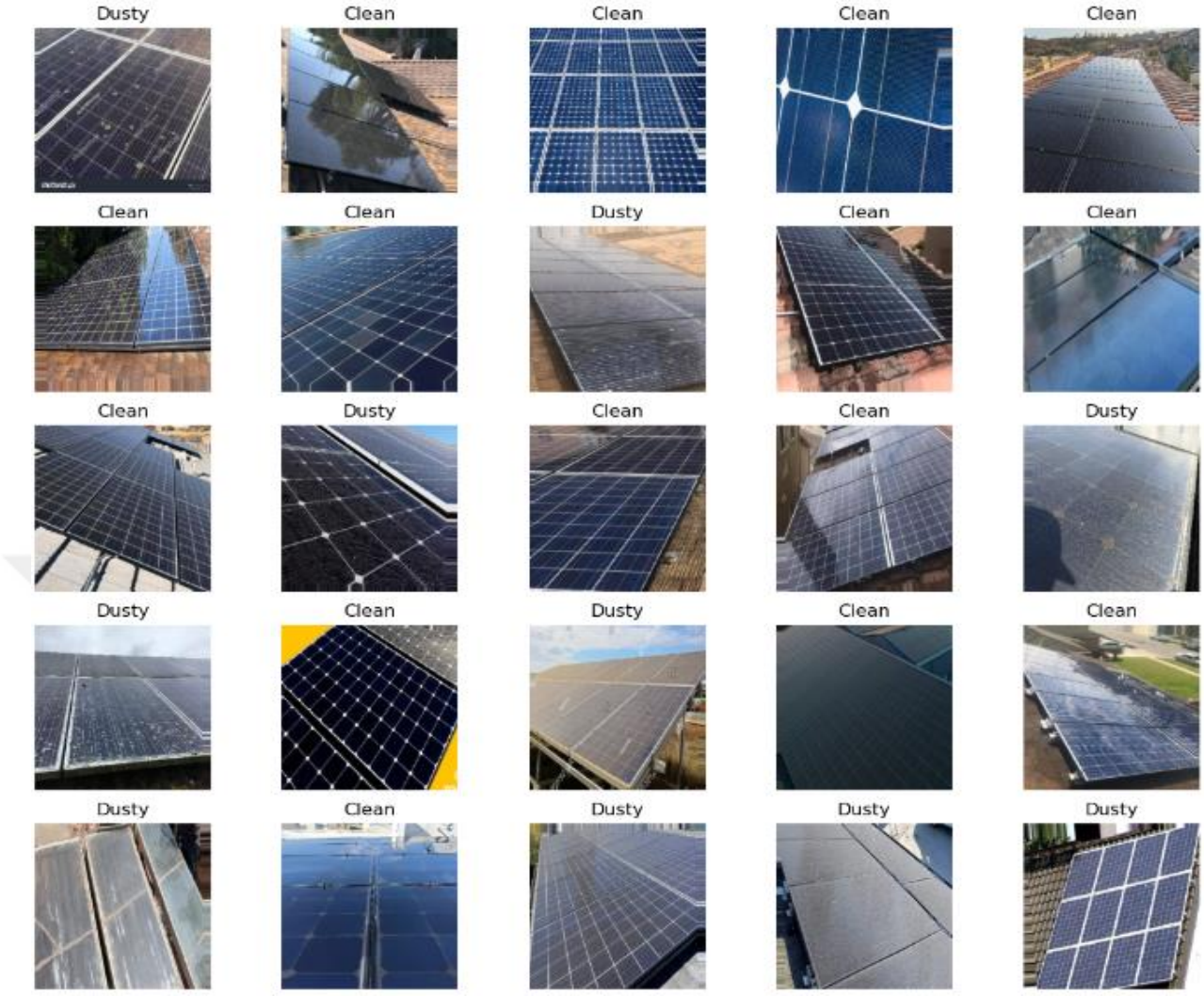

Figure 26. Samples of PV panel images dataset which randomly selected from clean and dust.

With use of the data preprocessing as:

- ✓ Data Cleaning: Eliminate duplicate or irrelevant images.
- ✓ Data Augmentation: Enhance the dataset using transformations (e.g., rotation, scaling) to improve model generalization.
- ✓ Image Filtering and Enhancement: Enhance the images by using suitable median filter.
- ✓ Data Normalizing: Dividing on the max gray level and hence produce images with pixel values between (0-1).
- ✓ Data Splitting: Splitting the dataset into training, validation, and testing sets.

The dataset was categorized into two classes namely clean, and dusty. During the training and validation processes 80% of total images (2049 images) were used, and

another 20% of total images (513 images) were used for validation and testing processes as (307 images) for validation and (206 images) for testing. The validation runs simultaneously with the training process to prevent model overfitting. Figure (2) shows the enhancement on a sample blurred image using median filter.

Blurred image Filtered image

Figure 27. The enhancement on a sample blurred image using median filter.

4.3 Training and Optimization

In the realm of deep learning and neural network optimization, training and fine-tuning models play a pivotal role in achieving optimal performance. This involves a multifaceted process encompassing model training, validation, hyperparameter tuning, and regularization. The Convolutional Neural Network (CNN) employed in this work undergoes rigorous training using a dataset, with parameters optimized through the Adam optimizer to maximize its efficiency. To ensure the model's generalizability and prevent overfitting, validation on a separate dataset becomes imperative.

• Model Training: Train the CNN model using the training dataset, optimizing parameters with Adam optimizer to maximize performance.

• Validation: Validate the model on the validation dataset to prevent overfitting.

• Hyperparameter Tuning: Fine-tune hyperparameters, including learning rate, batch size, and network architecture.

• Regularization: Implement dropout and L2 regularization to prevent overfitting.

In this work, the batch size for training is 16, so the epoch is 20 with 130 iteration each. The learning rate used is 0.001, while the momentum is 0.99.

4.4 Experimental Result

In order to develop the models with rich feature representations for a wide variety of PV-images, prevalent diverse data set is applied. We exploit four DL models which are:

- Inception v3
- VGG-16
- Resnet 50
- Proposed Net (called NetB0)

4.4.1 Inception v3 model

The Inception v3 model architecture is as shown in Figure (3).

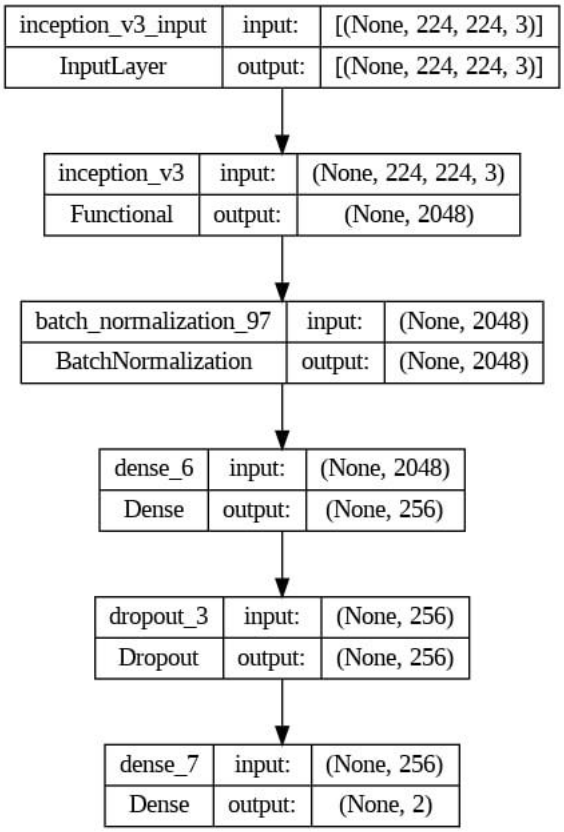

Figure 28. Inception v3 deep learning model structure.

The training and validation accuracy and loss curves within 20 epochs as depicted Figure (4).

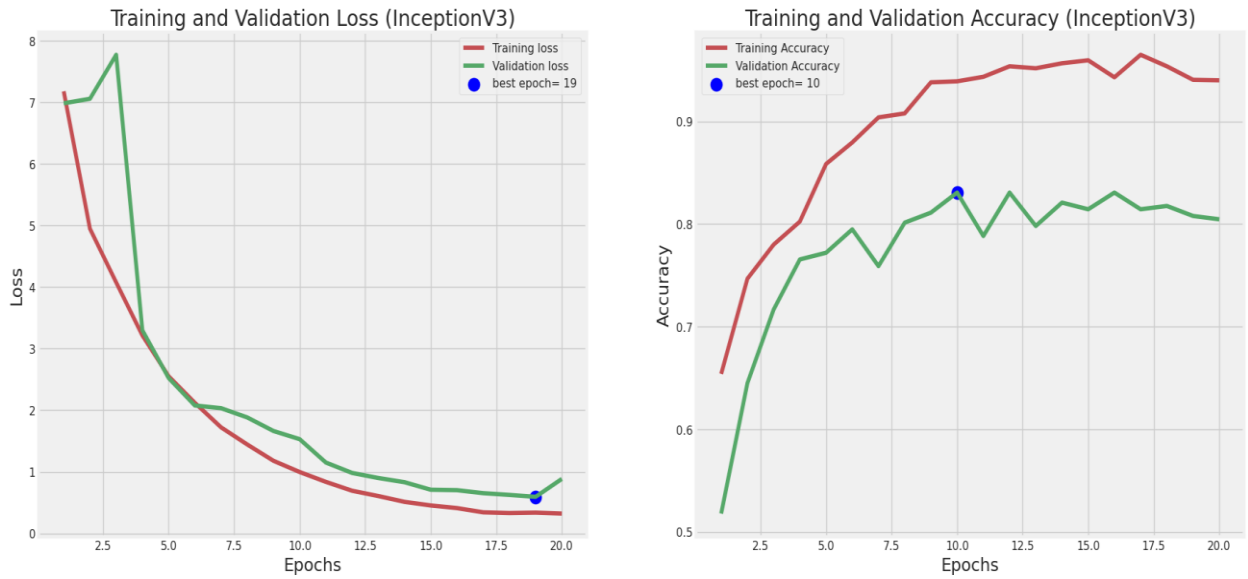

Figure 29. Inception v3 deep learning training curves.

The loss reaching less than 1 and the accuracy curves surpassing 90% for both training and validation sets suggest that the Inception V3 model has undergone successful training. The model's ability to achieve a low loss indicates effective convergence during training, while the high accuracy values for both the training and validation sets suggest that the model is performing well and generalizing adequately to unseen data. These trends indicate a robust and well-trained neural network.

The confusion matrix of Inception v3 of the testing images is as illustrated in Figure (5).

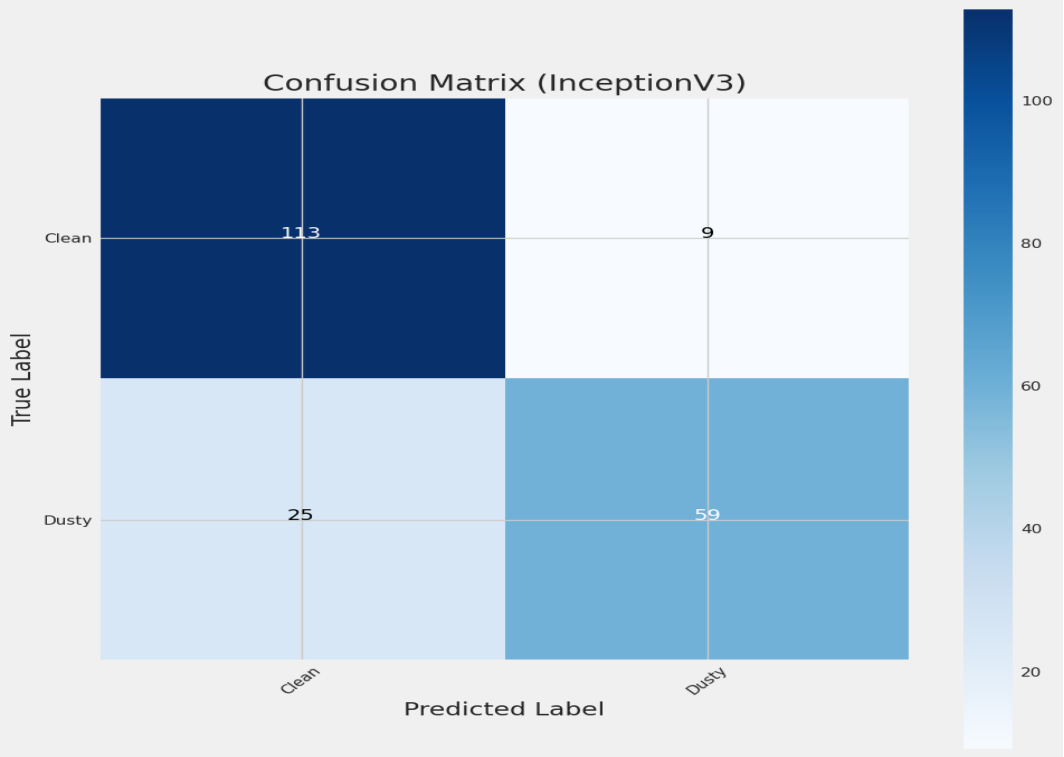

Figure 30. Inception v3 confusion matrix.

The confusion matrix provides a detailed breakdown of the model's classification performance. In this case, the matrix shows that for the "Clean" class, 113 instances were correctly classified, 9 instances were incorrectly classified as "Dusty," 25 instances of "Clean" were incorrectly classified as "Dusty," and 59 instances of "Dusty" were correctly classified. This matrix is instrumental in understanding the model's ability to distinguish between classes, offering insights into false positives and false negatives.

The assessment metrics of Inception v3 of the testing images is as illustrated in table (1).

Table 2. Evaluation metrics of the Inception v3

	Precision	**Recall**	**F-score**
Clean	84	93	88
Dusty	88	70	79
Accuracy	84	83	83

As in table above, Clean Class: The precision for the "Clean" class indicates that out of all instances predicted as "Clean," 84% were indeed true positives. This suggests a relatively low rate of false positives. The recall of 93% indicates that the model effectively captured 93% of all true "Clean" instances, minimizing false negatives. The F-score, a harmonic mean of precision and recall, provides a balanced measure of the model's performance, yielding a value of 88%. Dusty Class: For the "Dusty" class, the precision of 88% signifies that 88% of instances predicted as "Dusty" were true positives. The recall of 70% suggests that the model captured 70% of all true "Dusty" instances, indicating a relatively higher rate of false negatives compared to the "Clean" class. The F-score for the "Dusty" class is 79%, providing a combined measure of precision and recall. The overall accuracy of 83% indicates the proportion of correctly classified instances over the total instances. It offers a comprehensive view of the model's performance across both classes.

In summary, the Inception V3 model demonstrates strong performance with high accuracy and well-balanced evaluation metrics. However, it is essential to consider the specific application requirements and the relative importance of precision and recall depending on the consequences of false positives and false negatives in the context of the problem at hand.

4.4.2 Resnet 50 model

The Resnet 50 model architecture is as shown in Figure (6)

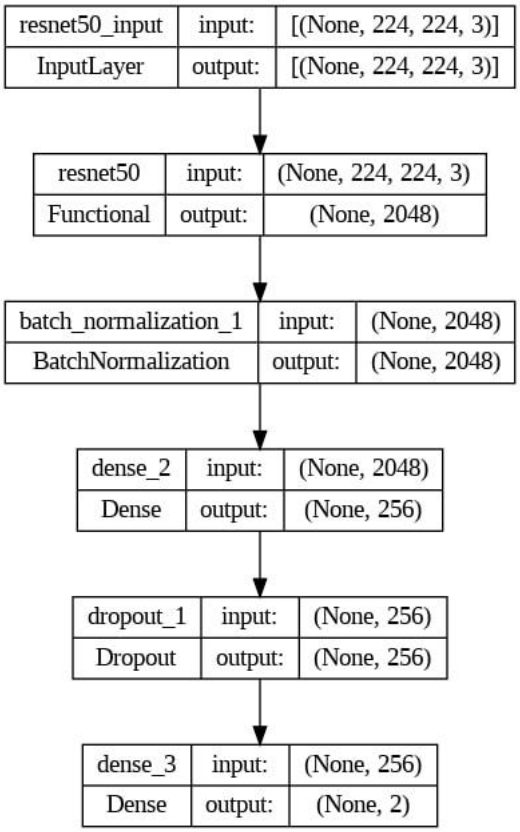

Figure 31. Resnet 50 deep learning model structure.

The training and validation accuracy and loss curves within 20 epochs as depicted Figure 23

Figure 32. Resnet 50 deep learning training curves.

The training process of the ResNet50 model is evident from the training and validation curves, with the loss reaching less than 3 and the training accuracy curve exceeding 95%, suggesting successful model convergence during training. However, the validation curve lagging below 85% raises concerns about potential overfitting, indicating that the model may be overly specialized to the training data and might struggle to generalize effectively to new, unseen data.

The confusion matrix of Resnet 50 of the testing images is as illustrated in Figure 33.

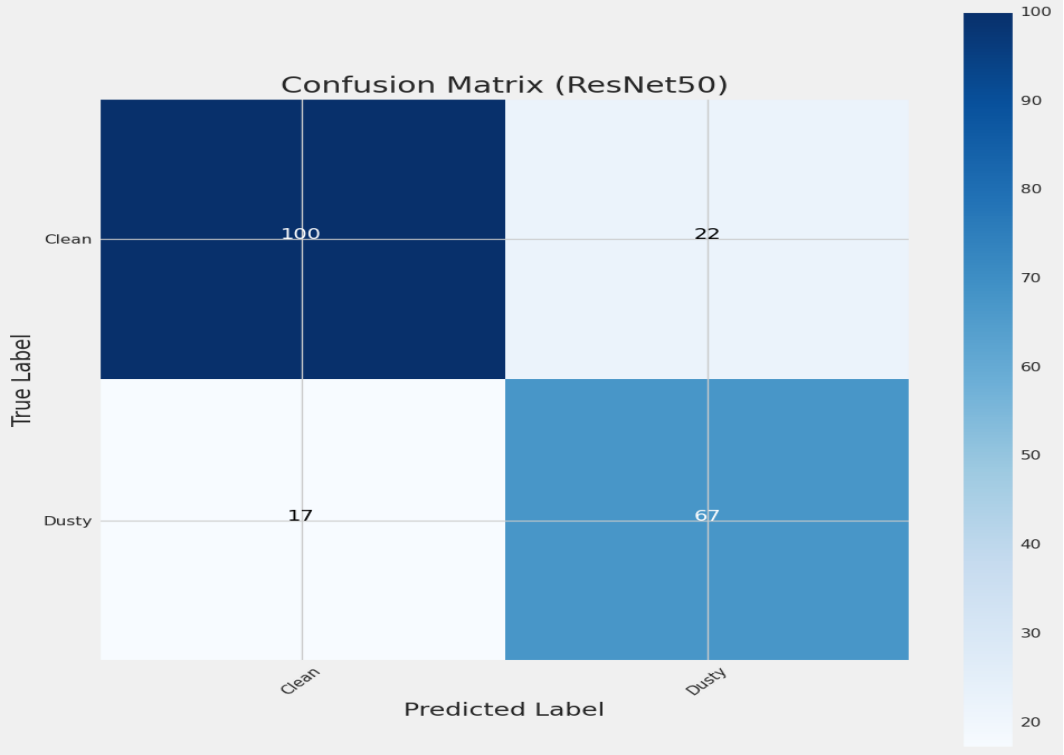

Figure 33. Resnet 50 confusion matrix.

The confusion matrix further elucidates the model's classification performance. In particular, it reveals that the model correctly classified 100 instances of the "Clean" class and 67 instances of the "Dusty" class. However, there were 22 instances of "Clean" misclassified as "Dusty" and 17 instances of "Dusty" misclassified as "Clean," underscoring the need for a balance between precision and recall.

The assessment metrics of resnet 50 of the testing images is as illustrated in Table (2).

Table 3. Evaluation metrics of the Resnet 50

	Precision	**Recall**	**F-score**
Clean	85	82	84
Dusty	75	80	77
Accuracy	80	81	81

Analyzing the evaluation metrics provides a detailed understanding of the model's performance in each class. For the "Clean" class, the precision of 85% indicates that 85% of instances predicted as "Clean" were true positives, and the recall of 82% implies that the model captured 82% of all true "Clean" instances, resulting in an F-score of 84%. In the "Dusty" class, the precision of 75% signifies that 75% of instances predicted as "Dusty" were true positives, while the recall of 80% indicates that the model captured 80% of all true "Dusty" instances, yielding an F-score of 77%.

The overall accuracy of the model is 81%, providing a general assessment of its correctness across both classes. While the model exhibits a high accuracy during training, attention should be paid to its generalization capacity as indicated by the lower validation accuracy. The trade-off between precision and recall becomes crucial, especially in scenarios where false positives and false negatives have different consequences. Fine-tuning or regularization techniques may be considered to address potential overfitting and enhance the model's ability to generalize effectively.

4.4.3 VGG-16 model

The VGG-16 model architecture is as shown in Figure 34.

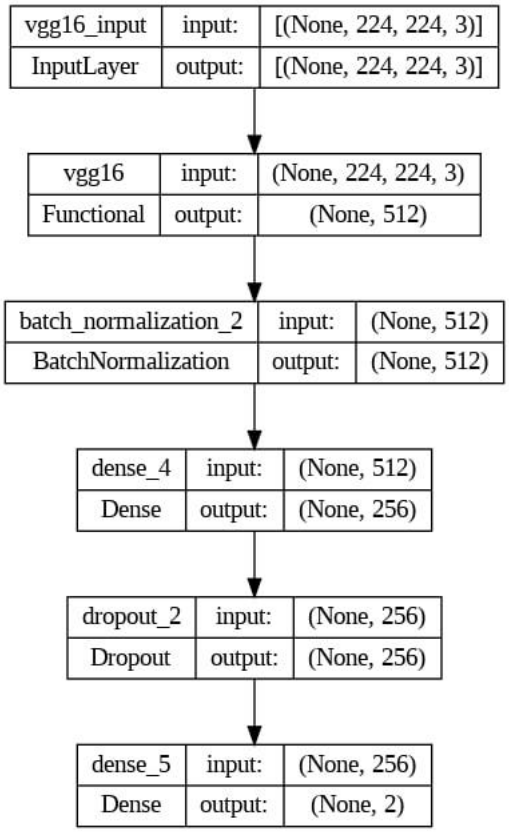

Figure 34.VGG-16 deep learning model structure.

The training and validation accuracy and loss curves within 20 epochs as depicted Figure 35.

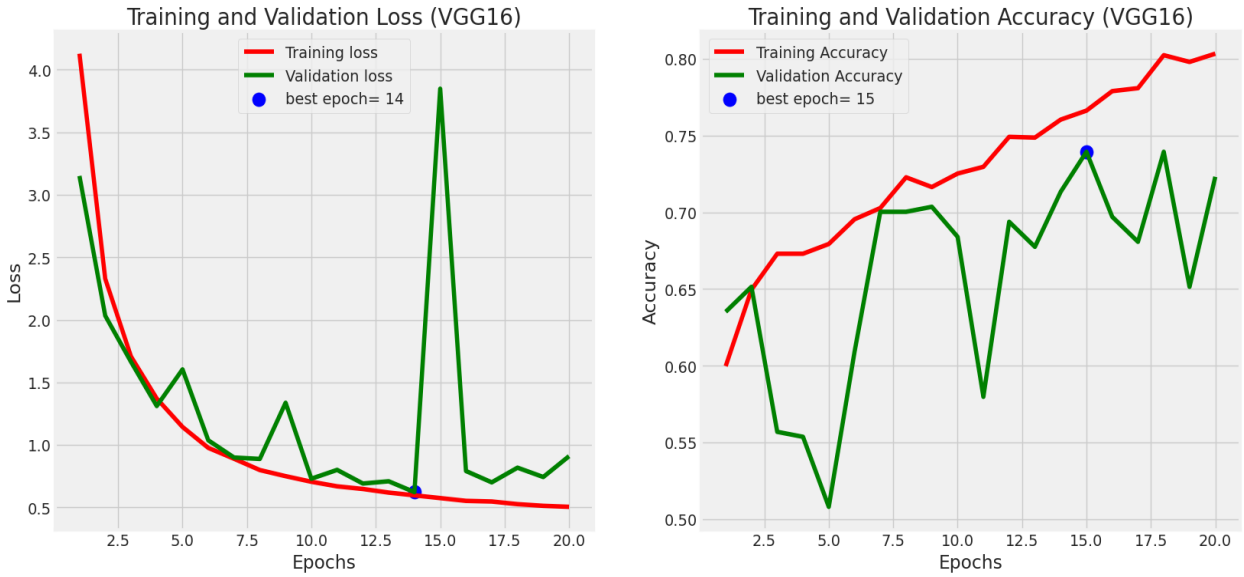

Figure 35. VGG-16 deep learning training curves.

The training and validation curves illustrate the training process of the VGG-16 model, with the loss reaching less than 1. However, the training accuracy curve falling below 80% and the validation curve below 75% suggest that the model might face challenges in achieving high accuracy and generalizing effectively to unseen data.

The confusion matrix of VGG of the testing images is as illustrated in Figure 36.

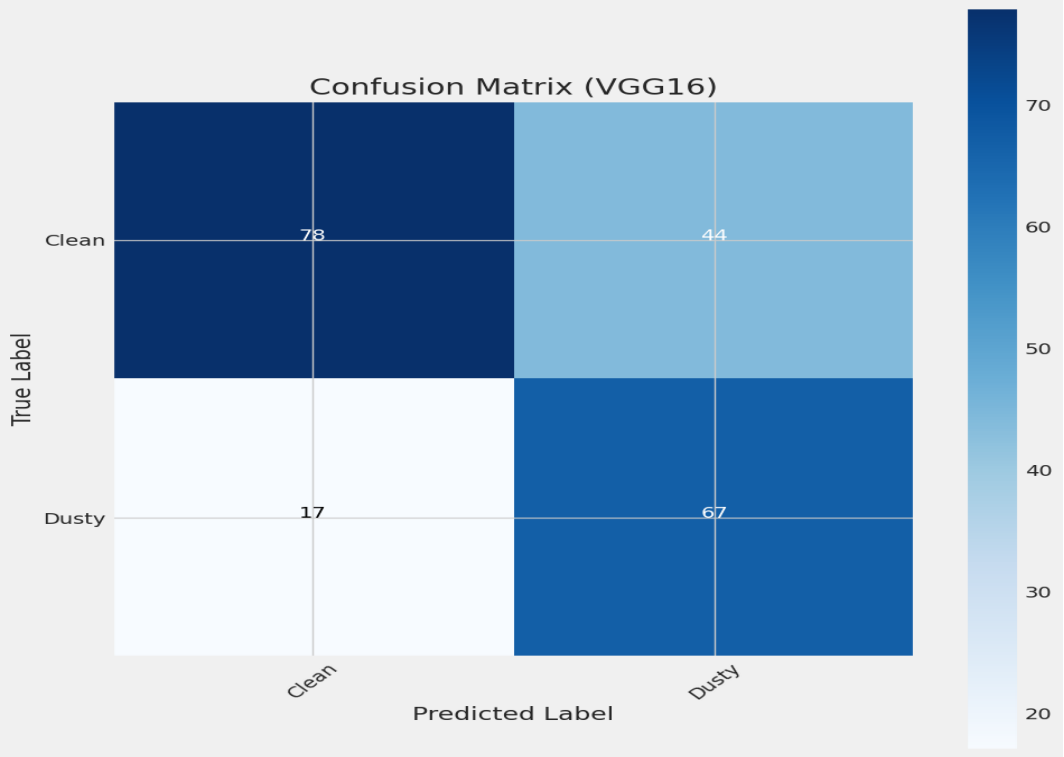

Figure 36. VGG-16 confusion matrix.

The confusion matrix delves into the classification performance, revealing that the model correctly classified 78 instances of the "Clean" class and 67 instances of the "Dusty" class. However, it also misclassified 44 instances of "Clean" as "Dusty" and 17 instances of "Dusty" as "Clean," indicating potential difficulties in distinguishing between the two classes.

The assessment metrics of VGG-16 of the testing images is as illustrated in Table (3).

Table 4. Evaluation metrics of the VGG-16

	Precision	**Recall**	**F-score**
Clean	82	64	73
Dusty	61	80	70
Accuracy	71	72	70

The training and validation curves illustrate the training process of the VGG-16 model, with the loss reaching less than 1. However, the training accuracy curve falling below 80% and the validation curve below 75% suggest that the model might face challenges in achieving high accuracy and generalizing effectively to unseen data.

The confusion matrix delves into the classification performance, revealing that the model correctly classified 78 instances of the "Clean" class and 67 instances of the "Dusty" class. However, it also misclassified 44 instances of "Clean" as "Dusty" and 17 instances of "Dusty" as "Clean," indicating potential difficulties in distinguishing between the two classes.

The evaluation metrics offer a detailed breakdown of the model's performance for each class. For the "Clean" class, the precision of 82% indicates that 82% of instances predicted as "Clean" were true positives, while the recall of 64% suggests that the model captured 64% of all true "Clean" instances, resulting in an F-score of 73%. In the "Dusty" class, the precision of 61% signifies that 61% of instances predicted as "Dusty" were true positives, and the recall of 80% indicates that the model captured 80% of all true "Dusty" instances, yielding an F-score of 70%.

The overall accuracy of the model is 70%, providing a general assessment of its correctness across both classes. The challenges observed in the training and validation curves, along with the misclassifications in the confusion matrix, highlight areas where the model might benefit from further optimization or tuning to improve its performance, potentially through adjustments in hyperparameters or additional data preprocessing techniques.

4.4.4 Efficientnet-B0 model

The proposed DL model architecture is as shown in Figure 37.

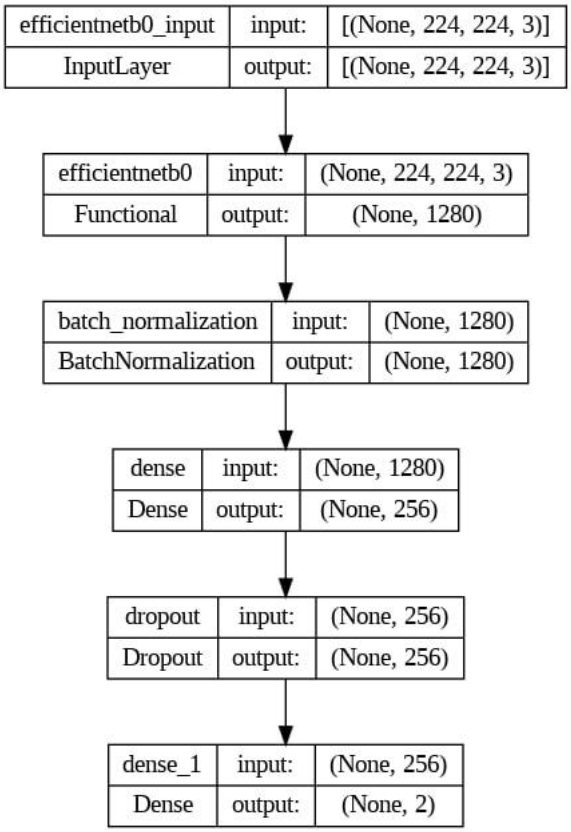

Figure 37. The proposed DL model structure.

Table 4 shows the proposed DL layers with their parameters.

Table 5. The proposed DL layers with their parameters.

Layer Type	Output Shape	Parameters
Efficientnet	(224,224,1280)	4049571
Batch Normalization	(244,244,1280)	5120
Dense_1	(None, 256)	327936
Dropout	(None, 256)	0
Dense_2	(None, 2)	512

The training and validation accuracy and loss curves within 20 epochs as depicted Figure 38.

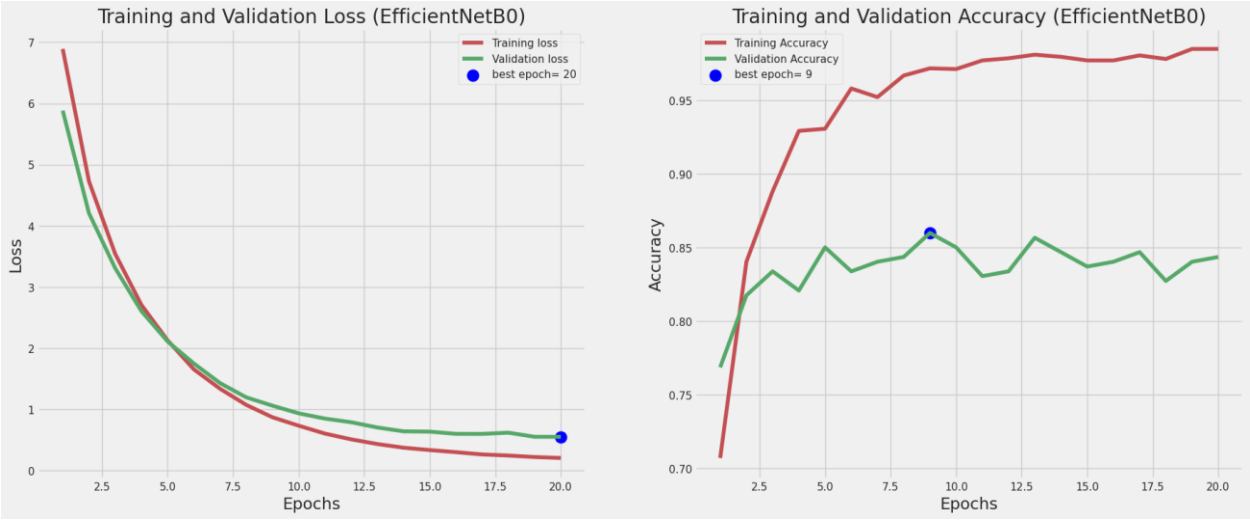

Figure 38. The proposed deep learning training curves.

The results for the proposed DL approach suggest a high level of training accuracy but potential challenges in generalization to the validation set. The training and validation curves reveal a well-converged model, with the loss reaching less than 0.5 and the training accuracy exceeding 97%. However, the validation curve lags behind at less than 85%, indicating potential overfitting and a need for caution regarding the model's ability to generalize to new data. The confusion matrix of proposed DL of the testing images is as illustrated in figure 39.

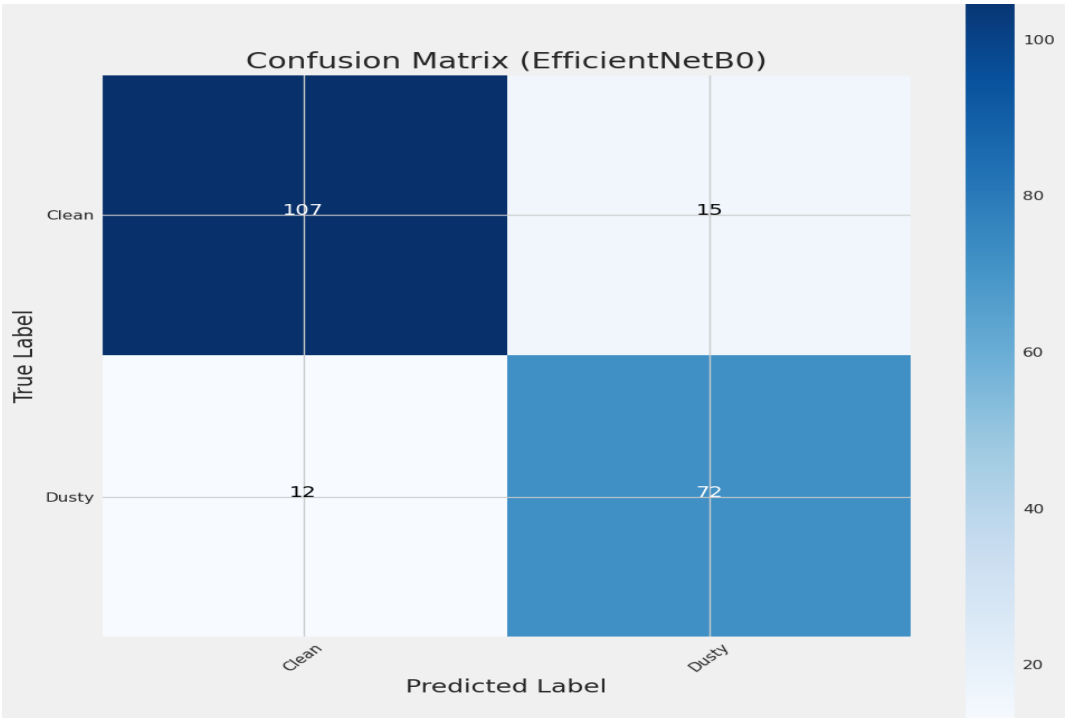

Figure 39. The proposed confusion matrix.

The confusion matrix provides a detailed classification breakdown, showcasing that the model correctly classified 107 instances of the "Clean" class and 72 instances of the "Dusty" class. However, it misclassified 15 instances of "Clean" as "Dusty" and 12 instances of "Dusty" as "Clean".

The assessment metrics of the proposed DL of the testing images is as illustrated in Table (5).

Table 6. Evaluation metrics of the proposed DL approach

	Precision	**Recall**	**F-score**
Clean	90	88	89
Dusty	84	86	85
Accuracy	86	87	87

The evaluation metrics offer further insights, with precision, recall, and F-score values indicating strong performance for both "Clean" and "Dusty" classes. The overall accuracy stands at 87%, emphasizing the model's correctness across both classes. Despite the high training accuracy, attention should be given to improving generalization, potentially through regularization techniques or adjusting model architecture, to ensure robust performance on unseen data.

The metric comparison models is as shown in Figure 40.

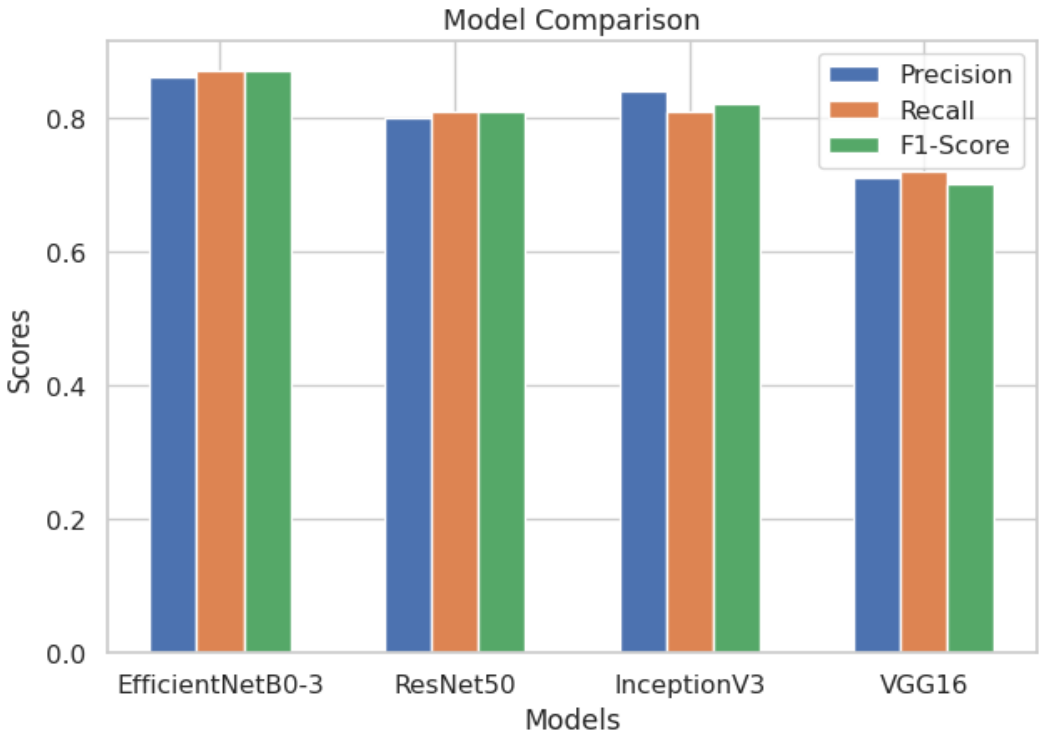

Figure 40. The metric comparison of all models.

The evaluation metric results indicate distinct performance characteristics among the four methods. The proposed DL approach demonstrates the highest overall accuracy at 87%, showcasing a balanced performance between precision, recall, and F-score for both "Clean" and "Dusty" classes. In comparison, Inception V3 achieves an accuracy of 83%, with strong precision and recall for the "Clean" class but slightly lower values for the "Dusty" class. ResNet50 exhibits an accuracy of 81%, with balanced precision and recall values for both classes. VGG-16, while achieving a moderate accuracy of 70%, displays challenges with precision and recall, especially for the "Clean" class. Overall, the proposed DL approach outperforms Inception V3, ResNet50, and VGG-16, demonstrating superior accuracy and balanced performance in classifying "Clean" and "Dusty" instances.

CONCULSION AND DICUSSION

Conclusion:

Solar panels, vital for converting sunlight into electricity, face efficiency challenges when accumulating dirt or debris. The severity of energy loss is contingent upon the level of dirt, with potential losses reaching up to 25%, according to the National Renewable Energy Laboratory. Additionally, dirty solar panels can expedite corrosion, diminishing the panels' lifespan. To address these challenges, regular cleaning, typically recommended twice a year, becomes crucial. The presented research introduces an intelligent dust detection system employing artificial intelligence, contributing to efficient solar panel maintenance and prolonged functionality in diverse weather conditions.

In summary, solar energy is a vital renewable resource, but dust accumulation on solar panels can significantly decrease their efficiency. Dust particles obstruct sunlight from reaching photovoltaic cells, reducing energy production. This problem is especially prevalent in arid regions. To address this issue, the project focuses on developing a robust dust detection system using deep learning and image processing. The dataset for this project is sourced from Kaggle, containing images of solar panel surfaces with varying dust levels.

The primary objectives of this project are:

- Develop a deep learning model for dust detection on solar panel surfaces.
- Achieve the highest detection accuracy using optimization algorithms like Deep Learning.
- Enhance module efficiency, reduce maintenance costs, and promote resource conservation.

DICUSSION

This thesis suggests detection and classification system using many robust deep learning approaches. It can recommend many valuable or applicable issues:

- Deploy the model for real-time dust detection and level estimation.
- Explore integration with robotic or automated cleaning systems.

- Estimate the level of dust on solar panels using image processing techniques.
- Expand the dataset to encompass diverse environmental conditions and dust types.
- Collaborate with solar panel manufacturers to implement the solution at scale.
- After dust detection, additional image processing steps will be taken to estimate dust levels, i.e, apply various image processing techniques to quantify the level of dust on solar panels.

REFERENCES

A. Dey, “Machine learning algorithms: a review,” International Journal of Computer Science and Information Technologies, vol. 7, no. 3, pp. 1174–1179, 2016.

A. G. Howard, M. Zhu, B. Chen, D. Kalenichenko, W. Wang, T. Weyand, M. Andreetto, and H. Adam, “Mobilenets: Efficient convolutional neural networks for mobile vision applications,” arXiv preprint arXiv:1704.04861, 2017.

A. J. Qasim and F. Q. A. Alyousuf, “History of Image Digital Formats Using in Information Technology,” QALAAI ZANIST SCIENTIFIC JOURNAL, vol. 6, no. 2, pp. 1098–1112, 2021.

A. Gupta, D. Goyal, and N. Hemrajani, “Performance Analysis of Various Video Compression Techniques,” International Journal of Science and Research, vol. 2, no. 8, pp. 335–338, 2013.

A. Khan, A. Sohail, U. Zahoora, and A. S. Qureshi, “A survey of the recent architectures of deep convolutional neural networks,” Artificial Intelligence Review, vol. 53, no. 8, pp. 5455–5516, 2020.

R. S. Sinha and S.-H. Hwang, “Comparison of CNN applications for RSSI-based fingerprint indoor localization,” Electronics, vol. 8, no. 9, p. 989, 2019.

A. M. Hambal, Z. Pei, and F. L. Ishabailu, “Image noise reduction and filtering techniques,” International Journal of Science and Research (IJSR), vol. 6, no. 3, pp. 2033–2038, 2017.

C. Luo, X. He, J. Zhan, L. Wang, W. Gao, and J. Dai, “Comparison and benchmarking of AI models and frameworks on mobile devices,” arXiv preprint arXiv:2005.05085, 2020.

A. Mathew, P. Amudha, and S. Sivakumari, “Deep Learning Techniques: An Overview,” in International Conference on Advanced Machine Learning Technologies and Applications, 2020, pp. 599–608.

A. Olaode, G. Naghdy, and C. Todd, “Unsupervised classification of images: A review,” International Journal of Image Processing, vol. 8, no. 5, pp. 325–342, 2014.

Abuqaaud, K. A., & Ferrah, A. (2020, February). A novel technique for detecting and monitoring dust and soil on solar photovoltaic panel. In 2020 Advances in Science and Engineering Technology International Conferences (ASET) (pp. 1-6). IEEE.

Adıgüzel, E., Özer, E., Akgündoğdu, A., & Yılmaz, A. E. (2019). Prediction of dust particle size effect on efficiency of photovoltaic modules with ANFIS: An experimental study in Aegean region, Turkey. Solar Energy, 177, 690-702.

Al Jaber, S. A. (2021). "RENEWABLES 2012 global status report". Renewable Energy Policy Network for the 21st Century.

Alfaris, F. E. (2023). A Sensorless Intelligent System to Detect Dust on PV Panels for Optimized Cleaning Units. Energies, 16(3), 1287.

B. K. Bose, "Global warming: Energy, environmental pollution, and the impact of power electronics," IEEE Ind. Electron. Mag., vol. 4, no. 1, pp. 6–17, 2010.

C. H. Lampert and C. Lampert, Kernel methods in computer vision. Now Publishers Inc, 2009. [48] J. E. Solem, Programming Computer Vision with Python: Tools and algorithms for analyzing images. O'Reilly Media, Inc., 2012.

Cipriani, G., D'Amico, A., Guarino, S., Manno, D., Traverso, M., & Di Dio, V. (2020). Convolutional neural network for dust and hotspot classification in PV modules. Energies, 13(23), 6357.

Cruz-Rojas, T., Franco, J. A., Hernandez-Escobedo, Q., Ruiz-Robles, D., & Juarez-Lopez, J. M. (2023). A novel comparison of image semantic segmentation techniques for detecting dust in photovoltaic panels using machine learning and deep learning. Renewable Energy, 217, 119126.

E. Beauxis-Aussalet and L. Hardman, "Visualization of confusion matrix for non-expert users," 2014.

E. Irmak and A. H. Ertas, "A review of robust image enhancement algorithms and their applications," in 2016 IEEE Smart Energy Grid Engineering (SEGE), 2016, pp. 371–375.

E. Kabalci, G. Gokkus, and A. Gorgun, "Design and implementation of a PI-MPPT based Buck-Boost converter," in 2015 7th International Conference on Electronics, Computers and Artificial Intelligence (ECAI), 2015, p. SG-23.

F. Famoso, R. Lanzafame, S. Maenza, and P. F. Scandura, "Performance comparison between micro-inverter and string-inverter Photovoltaic Systems," Energy Procedia, vol. 81, pp. 526–539, 2015.

Fan, S., Wang, X., Wang, Z., Sun, B., Zhang, Z., Cao, S., ... & Wang, Y. (2022). A novel image enhancement algorithm to determine the dust level on photovoltaic (PV) panels. Renewable energy, 201, 172-180.

Fan, S., Wang, Y., Cao, S., Zhao, B., Sun, T., & Liu, P. (2022). A deep residual neural network identification method for uneven dust accumulation on photovoltaic (PV) panels. Energy, 239, 122302.

G. Bonaccorso, Machine learning algorithms. Packt Publishing Ltd, 2017.

G. Zaccone, M. R. Karim, and A. Menshawy, Deep learning with TensorFlow. Packt Publishing Ltd, 2017.

H. Gholamalinezhad and H. Khosravi, "Pooling Methods in Deep Neural Networks, a Review," arXiv preprint arXiv:2009.07485, 2020.

H. Nguyen, "Fast object detection framework based on MobileNetV2 architecture and enhanced feature pyramid," Journal of Theoretical and Applied Information Technology, vol. 98, no. 05, 2020.

Jäger-Waldau, A. (2021). Snapshot of photovoltaics - March 2021. EPJ Photovoltaics, 12. https://doi.org/10.1051/epjpv/2021002

Jaszczur, M., Teneta, J., Styszko, K., Hassan, Q., Burzyńska, P., Marcinek, E., & Łopian, N. (2019). The field experiments and model of the natural dust deposition effects on photovoltaic module efficiency. Environmental Science and Pollution Research, 26, 8402-8417.

K. Sumithra, S. Buvana, and R. Somasundaram, "A Survey on Various Types of Image Processing Technique," International Journal of Engineering Research & Technology (IJERT) Vol, vol. 4, 2015.

L. El Chaar and N. El Zein, "Review of photovoltaic technologies," Renew. Sustain. energy Rev., vol. 15, no. 5, pp. 2165–2175, 2011. [11] F. Akarslan, "Photovoltaic systems and applications," Model. Optim. Renew. Energy Syst., p. 21, 2012.

M. D. Sontakke and M. S. Kulkarni, "Different types of noises in images and noise removing technique," International Journal of Advanced Technology in Engineering and Science, vol. 3, no. 1, pp. 102–115, 2015.

M. K. Khehra and M. Devgun, "Survey on Image Enhancement Techniques for Digital Images," Scholars Journal of Engineering and Technology (SJET), vol. 3, no. 2B, pp. 202–206, 2015.

M. Klein, T. Ralya, B. Pollak, R. Obenza, and M. G. Harbour, A practitioner's handbook for real-time analysis: guide to rate monotonic analysis for real-time systems. Springer Science & Business Media, 2012.

M. Mirhosseini, J. Pou, and V. G. Agelidis, "Single-and two-stage inverter-based grid-connected photovoltaic power plants with ridethrough capability under grid faults," IEEE Trans. Sustain. Energy, vol. 6, no. 3, pp. 1150–1159, 2014.

M. N. Mustafa, "Design of a grid connected photovoltaic power electronic converter," Master thesis, The artctic university of norway, 2017.

M. Sandler, A. Howard, M. Zhu, A. Zhmoginov, and L.-C. Chen, "Mobilenetv2: Inverted residuals and linear bottlenecks," in Proceedings of the IEEE conference on computer vision and pattern recognition, 2018, pp. 4510–4520.

Maity, R., Shamaun Alam, M., & Pati, A. (2020). An Approach for Detection of Dust on Solar Panels Using CNN from RGB Dust Image to Predict Power Loss. Cognitive Computing in Human Cognition: Perspectives and Applications, 41-48.

Masoom, A., Kosmopoulos, P., Bansal, A., Gkikas, A., Proestakis, E., Kazadzis, S., & Amiridis, V. (2021). Forecasting dust impact on solar energy using remote sensing and modeling techniques. Solar Energy, 228, 317-332.

Messenger, R. A., & Abtahi, A. (2018). Photovoltaic systems engineering. CRC press.

Mohammad Reza Maghami, Hashim Hizam, Chandima Gomes, Mohd Amran Radzi, Mohammad Ismael Reza dad, Shahrooz Hajighorbani, "Power loss due to soiling on solar panel: Areview", Renewable and Sustain able Energy Reviews 59 (2016) 1307–1316.

Mohammed, H. A., Baha'a, A. M., & Al-Mejibli, I. S. (2018, May). Smart system for dust detecting and removing from solar cells. In Journal of Physics: Conference Series (Vol. 1032, No. 1, p. 012055). IOP Publishing.

N. L. Panwar, S. C. Kaushik, and S. Kothari, "Role of renewable energy sources in environmental protection: A review," Renew. Sustain. energy Rev., vol. 15, no. 3, pp. 1513–1524, 2011.

O. P. Mahela and A. G. Shaik, "Comprehensive overview of grid interfaced solar photovoltaic systems," Renew. Sustain. Energy Rev., vol. 68, pp. 316–332, 2017.

Onim, M. S. H., Sakif, Z. M. M., Ahnaf, A., Kabir, A., Azad, A. K., Oo, A. M. T., & Ali, M. S. (2022). Solnet: A convolutional neural network for detecting dust on solar panels. Energies, 16(1), 155.

P. A. Laplante, "Real-time systems design and analysis," IEEE Press, New Jersey, United States, pp. 105- 130, 2004.

P. C. Sen, M. Hajra, and M. Ghosh, "Supervised classification algorithms in machine learning: A survey and review," in Emerging technology in modelling and graphics, Springer, 2020, pp. 99–111.

Qasem, H., Mnatsakanyan, A., & Banda, P. (2016, June). Assessing dust on PV modules using image processing techniques. In 2016 IEEE 43rd Photovoltaic Specialists Conference (PVSC) (pp. 2066-2070). IEEE.

Roumpakias, E.; Stamatelos, T. Surface Dust and Aerosol Effects on the Performance of Grid-Connected Photovoltaic Systems. Sustainability 2020, 12, 569.

S. Albawi, T. A. Mohammed, and S. Al-Zawi, "Understanding of a convolutional neural network," in 2017 International Conference on Engineering and Technology (ICET), 2017, pp. 1–6.

S. B. Kjaer, J. K. Pedersen, S. Member, and F. Blaabjerg, "A Review of Single-Phase Grid-Connected Inverters for Photovoltaic Modules," vol. 41, no. 5, pp. 1292–1306, 2005. content/uploads/2020/06/GTR_2020.pdf.

L. A. G. Rodriguez and J. C. Balda, "A comparison of isolated DC-DC converters for microinverter applications," in 2013 Twenty-Eighth Annual IEEE Applied Power Electronics Conference and Exposition (APEC), 2013, pp. 2084–2091.

S. Harb, M. Kedia, H. Zhang, and R. S. Balog, "Microinverter and string inverter grid-connected photovoltaic system—A comprehensive study," in 2013 IEEE 39th Photovoltaic Specialists Conference (PVSC), 2013, pp. 2885–2890.

S. Indolia, A. K. Goswami, S. P. Mishra, and P. Asopa, "Conceptual understanding of convolutional neural network-a deep learning approach," Procedia computer science, vol. 132, pp. 679–688, 2018.

S. Li and H. Zheng, "Energy extraction characteristic study of solar photovoltaic cells and modules," in 2011 IEEE Power and Energy Society General Meeting, 2011, pp. 1–7.

Saquib, D., Nasser, M. N., & Ramaswamy, S. (2020, August). Image Processing Based Dust Detection and prediction of Power using ANN in PV systems. In 2020 Third

International Conference on Smart Systems and Inventive Technology (ICSSIT) (pp. 1286-1292). IEEE.

Shaaban, M.F.; Alarif, A.; Mokhtar, M.; Tariq, U.; Osman, A.H.; Al-Ali, A.R. A New Data-Based Dust Estimation Unit for PV Panels. Energies 2020, 14, 3601.

Shubbak, M. H. (2019). Advances in solar photovoltaics: Technology review and patent trends. Renewable and Sustainable Energy Reviews, 115, 109383.

Styszko, K., Jaszczur, M., Teneta, J., Hassan, Q., Burzyńska, P., Marcinek, E., ... & Samek, L. (2019). An analysis of the dust deposition on solar photovoltaic modules. Environmental Science and Pollution Research, 26, 8393-8401.

T. Ibn-Mohammed et al., "Perovskite solar cells: An integrated hybrid lifecycle assessment and review in comparison with other photovoltaic technologies," Renew. Sustain. Energy Rev., vol. 80, pp. 1321–1344, 2017.

T. O. Ayodele, "Types of machine learning algorithms," New advances in machine learning, vol. 3, pp. 19–48, 2010.

U. R. Hodeghatta and U. Nayak, "Unsupervised Machine Learning," in Business Analytics Using R-A Practical Approach, Springer, 2017, pp. 161–186.

W. Xiao, Photovoltaic power system: modeling, design, and control. John Wiley & Sons, 2017.

A. Askarzadeh and A. Rezazadeh, "Parameter identification for solar cell models using harmony search-based algorithms," Sol. Energy, vol. 86, no. 11, pp. 3241–3249, 2012.

D. Rusirawan and I. Farkas, "Identification of model parameters of the photovoltaic solar cells," Energy Procedia, vol. 57, pp. 39–46, 2014.

Wu, Z.; Zhou, Z.; Alkahtani, M. Time-Effective Dust Deposition Analysis of PV Modules Based on Finite Element Simulation for Candidate Site Determination. IEEE Access 2020.

Y. Bengio, I. Goodfellow, and A. Courville, Deep learning, vol. 1. MIT press Massachusetts, USA:, 2017.

Y. Li and R. Oruganti, "A low cost flyback CCM inverter for AC module application," IEEE Trans. Power Electron., vol. 27, no. 3, pp. 1295–1303, 2011.

Yfantis, E.; Fayed, A. A Camera System for Detecting Dust And Other Deposits On Solar Panels. Adv. Image Video Process. 2014, 2, 1–10.

RESUME

Personal Information

Surname, name : Faten Jabbar Mahdi Al- Azzawi

Nationality : Iraq

Foreign Language : Arabic - English